

**THE REPUBLIC OF TURKEY İSTANBUL KÜLTÜR UNIVERSITY**

**INSTITUTE OF GRADUATE STUDIES**

**THE INFLUENCE OF LIQUID TANKS ON THE SEISMIC RESPONSE OF  
ISOLATED STRUCTURE**

**Master's Thesis of Applied Science**

**RAMEEN MIRZADA**

**ID: 1800005601**

**Department of Civil Engineering**

**Institute of Graduate Studies**

**Program: Structural Engineering**

**Thesis Supervisor: Assist. Prof. Dr. Gökhan Yazıcı**

**SEPTEMBER 2022**

**T.C.**  
**İSTANBUL KÜLTÜR UNIVVERSİTY**  
**INSTITUTE OF GRADUATE STUDIES**

**THE INFLUENCE OF LIQUID TANKS ON THE SEISMIC RESPONSE OF  
ISOLATED STRUCTURE**

**Master's Thesis of Applied Science**

**RAMEEN MIRZADA**

**ID: 1800005601**

**Date of submission: 6/09/2022**

**Date of defense examination: 19/09/200**

**Department: Civil Engineering**

**Program: Structural Engineering**

**Supervisor and Chairperson:**

**Assist. Prof. Dr. Gökhan YAZICI**

**Members of Examining Committee:**

**Prof. Dr. Necmettin GÜNDÜZ**

**Assist. Prof. Dr. Erdal COŞKUN**

## **ACKNOWLEDGEMENT**

In the name of Allah, the most gracious and the most merciful, First and foremost, I am thankful to Almighty Allah for giving me the strength, ability, knowledge, and opportunity to undertake this study and complete it successfully.

Secondly, I would like to acknowledge and give my warmest thanks to my supervisor, Assist. Prof. Dr. Gökhan Yazıcı made this work possible. His guidance and advice carried me through all the stages of writing my thesis project. I would also like to thank my committee members for letting my defense be an enjoyable moment and for your thoughtful comments and suggestions; thank you.

Finally, I would also like to give special thanks to my mother and my family for their continuous support and understanding throughout my research and writing my thesis project.

**University:** İstanbul Kültür University

**Institute:** Institute of Graduate Studies

**Department:** Civil Engineering

**Program:** Structural Engineering

**Supervisor:** Assist. Prof. Dr. Gökhan Yazıcı

## **ABSTRACT**

This study investigates the influence of liquid tanks on the seismic response of a Lead Rubber Bearing isolated structure under six near-fault ground excitations. Liquid tanks with various sizes and aspect ratios located on the base floor were used to assess the effect of sloshing on the seismic response. The response history analysis of the building model was performed with a MATLAB script. The sloshing effect of liquid was considered by using a mechanical modeling of liquid tanks with rigid walls. The structural response was analyzed using the selected ground acceleration records. The response parameters, such as hysteresis loops, bearing displacement, story drift of the structure, and liquid sloshing displacements, were investigated. The analysis results show that large bearing displacements were observed for building models with slender tanks subjected to earthquakes with high Peak Ground Displacements (PGD).

**Keywords:** Liquid Tanks, Seismic Isolation, Lead Rubber Bearing, Response History Analysis, Hysteresis loops, Bearing displacement.

**Üniversite: İstanbul Kültür Üniversitesi**

**Enstitüsü: Lisansüstü Eğitimi Enstitüsü**

**Anabilim Dalı: İnşaat Mühendisliği**

**Programı: Yapı (İngilizce)**

**Tez Danışmanı: Dr. Öğretim Üyesi Gökhan Yazıcı**

## **ÖZET**

Bu çalışma, sıvı tanklarının altı yakın fay deprem ivme kaydına maruz kurşun çekirdekli kauçuk mesnetli bir yapının sismik tepkisi üzerindeki etkisini araştırmaktadır. Çalkalanmanın sismik tepki üzerindeki etkisini değerlendirmek için taban zemine yerleştirilmiş çeşitli boyut ve en boy oranlarına sahip sıvı tankları kullanılmıştır. Bina modelinin sismik davranış analizi bir MATLAB betiği ile gerçekleştirilmiştir. Sıvının çalkalama etkisi, rijit duvarlı sıvı tankları için geliştirilen bir mekanik model kullanılarak değerlendirilmiştir. Yapısal tepki, seçilen yer ivmesi kayıtları kullanılarak analiz edilmiştir. Histeresis çevrimleri, mesnet yer değiştirmesi, yapının kat ötelenmesi ve sıvı çalkantı yer değiştirmeleri gibi tepki parametreleri incelenmiştir. Analiz sonuçları, yüksek Pik Yer Değiştirmesi olan depremlere maruz kalan ve boy/en oranı yüksek tanklı bina modellerinde büyük mesnet yer değiştirmelerinin gözlemlendiğini göstermektedir.

**Anahtar Kelimeler:** Sıvı Tankları, Sismik İzolasyon, Kurşun Çekirdekli Kauçuk Mesnet, Tepki Geçmiş Analizi, Histeresis döngüleri, Mesnet Yerdeğiştirmesi.

# TABLE OF CONTENTS

<b>ABSTRACT .....</b>	<b>ii</b>
<b>ÖZET .....</b>	<b>iii</b>
<b>TABLE OF CONTENTS.....</b>	<b>iv</b>
<b>LIST OF TABLES.....</b>	<b>ix</b>
<b>LIST OF FIGURES .....</b>	<b>x</b>
<b>LIST OF SYMBOLS AND NOTATIONS.....</b>	<b>vii</b>
<b>CHAPTER 1 .....</b>	<b>1</b>
<b>INTRODUCTION .....</b>	<b>1</b>
1.1 Introduction.....	1
1.2 Motivation.....	2
1.3 Literature Review .....	2
1.4 Research Objectives and Aim of The Thesis .....	7
1.5 Overview of the Thesis Structure.....	8
<b>CHAPTER 2 .....</b>	<b>10</b>
<b>SEISMIC ISOLATION SYSTEMS.....</b>	<b>10</b>
2.1 Overview.....	10
2.2 Working Principle of Seismic Isolation System .....	10
2.3 Types of Seismic Isolation.....	11
2.4 Sliding Bearing.....	12
2.4.1 Flat Sliding .....	12
2.4.2 Friction pendulum system (FPS) .....	12
2.5 Elastomeric Bearing Isolator.....	13
2.5.1 Low Damping Rubber Bearings .....	13

2.5.2 High Damping Rubber Bearings .....	13
2.5.3 Lead Rubber Bearing Isolator.....	14
2.5.4 Properties of Lead Rubber Bearing Isolator .....	15
2.6 Modeling and Parameters of Lead Rubber Bearing .....	16
<b>CHAPTER 3 .....</b>	<b>18</b>
LIQUID STORAGE TANKS SUBJECTED TO EARTHQUAKE EXCITATION ...	18
3.1 Overview .....	18
3.2 Fundamentals of Liquid Sloshing .....	18
3.3 Mechanical Modeling of Liquid Storage Tanks .....	19
3.3.1 Mechanical Analogue for Tanks Case One .....	22
3.3.2 Mechanical Analogue of Liquid Tanks Case Two .....	24
3.3.3 Mechanical Analogue of Liquid Tanks Case Three .....	25
<b>CHAPTER 4 .....</b>	<b>27</b>
NUMERICAL STRUDY .....	27
4.1 Description of the Isolated Structure.....	27
4.2 Analysis of the Model and Governing Equations of Motions .....	28
4.3 Selection of the Ground Motion Records .....	31
<b>CHAPTER 5 .....</b>	<b>34</b>
RESULTS AND DISCUSSION .....	34
5.1 Results and Discussion .....	34
5.1.1 Liquid Tank Model One .....	34
5.1.2 Bearing Force .....	34
5.1.3 Bearing Displacement .....	35
5.1.4 Story Drift.....	36
5.1.5 Liquid Tank Model Two and Three.....	38

5.1.6 Bearing Force .....	38
5.1.7 Bearing Displacement .....	39
5.1.8 Story Drift.....	39
5.1.9 Sloshing Displacement of Liquid .....	40
<b>CHAPTER 6 .....</b>	<b>42</b>
6.1 conclusion .....	42
6.2 Recommendation For Future Studies .....	43
<b>APPENDIX A .....</b>	<b>43</b>
<b>REFERENCES .....</b>	<b>44</b>
<b>APPENDIX B.....</b>	<b>47</b>
Case One.....	47
Case Tow .....	56
Case Three .....	61

## LIST OF SYMBOLS AND NOTATIONS

<b>LT1:</b> -	liquid tank number one
<b>LT2:</b> -	liquid tank number two
<b>LT3:</b> -	liquid tank number three
<b>LT4:</b> -	liquid tank number four
<b>LT5:</b> -	liquid tank number five
<b>LT6:</b> -	liquid tank number six
<b>LT6R:</b> -	liquid tank number seven
<b>LT8:</b> -	liquid tank number eight
<b>LT9:</b> -	liquid tank number nine
<b>LT10:</b> -	liquid tank number ten
<b>LT11:</b> -	liquid tank number eleven
<b>TLD:</b> -	Tuned liquid damper
<b>TLCD:</b> -	Tuned liquid column damper
<b>TMD:</b> -	Tuned Mass Damper
<b>m:</b> -	Mass of the super-structure
<b>m:</b> -	Total mass of the liquid tank
<b>m<sub>b</sub>:</b> -	Mass of the base/bearing
<b>m<sub>c</sub>:</b> -	Convective mass of liquid
<b>m<sub>i</sub>:</b> -	Impulsive mass of liquid
<b>L:</b> -	Inside length of rectangular tank parallel to the direction of seismic force
<b>K<sub>s</sub>:</b> -	Lateral stiffness of columns in the super-structure

<b><math>K_c</math>:</b> -	Lateral stiffness of convective mass inside the tank
<b><math>C</math>:</b> -	Damping coefficient of the structure
<b><math>C_c</math>:</b> -	Damping coefficient of convective mass of liquid
<b><math>m_t</math>:</b> -	Mass of empty tank
<b><math>m_w</math>:</b> -	Total mass of water
<b><math>g</math>:</b> -	Acceleration due to gravity
<b><math>h</math>:</b> -	Maximum depth of liquid
<b><math>h_c</math>:</b> -	Height of convective mass above the bottom of the tank
<b><math>h_i</math>:</b> -	Height of impulsive mass above the bottom of the tank wall
<b><math>H</math>:</b> -	Height of tank
<b><math>B</math>:</b> -	Width of the tank
<b>ERB:</b> -	Elastomeric rubber bearing
<b>LRB:</b> -	Lead rubber bearing
<b>ACI:</b> -	American concrete institute
<b>ASCE:</b> -	American Society of Civil Engineering

## LIST OF TABLES

<b>Table 3.1</b> Model Parameters of Liquid Storage Tanks .....	23
<b>Table 3.2</b> Model Parameters of Liquid Storage Tanks for First Option .....	25
<b>Table 3.3</b> Parameters of Liquid Storage Tanks .....	26
<b>Table 4.1</b> Lists of Features of Six Near-Fault Ground Excitation .....	31
<b>Table 5.1</b> Maximum Response Of (LT1 to LT5) for Six Near-Fault Earthquakes .....	37
<b>Table 5.2</b> Maximum Response Of (LT6 to LT8) for Six Near-Fault Earthquakes .....	41
<b>Table 5.3</b> The Response of Isolated Structure with Tanks Model 3 .....	41

## LIST OF FIGURES

<b>Figure 2.1</b> Effect of Seismic Base Isolation [35].....	10
<b>Figure 2.2</b> Influence of Period Shift of Base Isolated Structure [19]. .....	11
<b>Figure 2.3</b> Typical Hysteresis Loops for Elastomeric Bearings [36] .....	14
<b>Figure 2.4</b> Lead Rubber Bearing Isolator [21]. .....	15
<b>Figure 2.5</b> Force Displacement Hysteresis Loop of Lead Rubber Bearing [21]. .....	15
<b>Figure 2.6</b> Restoring Force of Isolated Bearing [22] .....	16
<b>Figure 3.1</b> Distribution of impulsive hydrodynamic pressures [27].....	19
<b>Figure 3.2</b> Distribution of convective hydrodynamic pressures [27]. .....	19
<b>Figure 3.3</b> Spring Mass Model for Circular and Rectangular Tanks [29]. .....	21
<b>Figure 3.4</b> Mechanical Analogue of Liquid Tank Case One.....	23
<b>Figure 3.5</b> Liquid Tanks LT1, LT2, LT3, LT4, LT5 .....	23
<b>Figure 3.6</b> Mechanical Analogue of Liquid Tank case two .....	24
<b>Figure 3.7</b> Liquid Tanks case two.....	24
<b>Figure 3.8</b> Mechanical Analogue of Liquid Tanks case 2 .....	25
<b>Figure 3.9</b> Liquid Tanks for Case Two .....	25
<b>Figure 4.1</b> Schematics Model of Isolated Structure with Liquid Tank.....	28
<b>Figure 4.2</b> Ground Acceleration Time History Centro Array #9 .....	32
<b>Figure 4.3</b> Ground Acceleration Time History of Izmit,90.....	32
<b>Figure 4.4</b> Ground Acceleration Time History of Northridge-01 Med Ff, 90 .....	32
<b>Figure 4.5</b> Ground Acceleration Time History of Cape Mendocino, 270 .....	33
<b>Figure 4.6</b> Ground Acceleration Time History of Chi-Chi, Tcu067, EW .....	33

<b>Figure 4.7</b> Ground Acceleration Time History of Iwate, Myg004, Ew .....	33
<b>Figure 5.1</b> Response of Isolated Building with Liquid Tanks.....	35
<b>Figure 5.2</b> Response of Isolated Building with Liquid Tanks Model 1.....	36
<b>Figure 5.3</b> Response of Isolated Building with Liquid Tanks Model 1.....	37
<b>Figure 5.4</b> Response of Isolated Building with Liquid Tanks Model 2 And 3 .....	38
<b>Figure 5.5</b> Response of Isolated Building with Liquid tanks case two.....	39
<b>Figure 5.6</b> Response of Isolated Structure with Liquid tanks case two .....	39
<b>Figure 5.7</b> Response of Isolated Building with Liquid Tanks Model 2.....	40

# CHAPTER 1

## INTRODUCTION

### 1.1 Introduction

Seismic isolation is an effective method of reducing the damaging effect of severe earthquakes on structural systems and nonstructural elements [41]. However, it is an old theory that has recently gained worldwide acceptance because of recent developments in base isolation technology. The primary concept of base isolation is to isolate the super-structure from its base by providing a horizontally flexible layer of isolation bearings. Therefore, super-structure is decoupled from the foundation, leading to mitigation of ground acceleration and lateral forces to be transferred to the super-structure. [1]

In seismic isolated structures, the displacement caused due earthquakes is concentrated mainly at isolators, and the super-structure behaves like a rigid block; therefore, the relative displacement (inter-story drift) is reduced significantly. By restricting the inelastic response to the isolators, therefore isolated structures may be designed to behave almost or perfectly elastic. [18]

The components of the super-structure may typically be designed for less force than the components of the same structure without an isolation system since the isolation system minimizes the forces conveyed to the super-structure; this would reduce the initial expenses, which might cover the cost associated with the installation of the seismic isolation system. Overall, seismic isolation gives a reduced life-cycle price taking into consideration the reduction of repair, and retrofitting expenditures related to earthquake damage [1].

The first innovative design of seismic isolation system was proposed by Touaillon in 1870. His design approach was to build a super-structure on spherical balls which allowed free movement in the horizontal direction [2]. Over the years, different types of isolation systems were developed, such as sliding bearings (flat sliding bearings, spherical sliding

bearings) and elastomeric bearings (low-damping bearings, high-damping natural rubber bearings (HDRB), lead rubber bearings (LRB)).

Liquid tanks are vitally essential structures that are constructed to serve a wide range of functions, including storing various kinds of liquid, such as water for drinking and fire-extinguishing, oil, chemical fluids, and natural gas. They also have critical applications such as storage containers in nuclear power plants. There has been comprehensive research on the damping properties of liquid tanks, especially the sloshing liquid storage tanks. [42]

Researchers observed that the sloshing behavior of liquid storage tanks could act as a damping device and might assist in controlling the seismic response of buildings. Recently Anupam Das investigated the response of a deep liquid storage tank installed on the roof of a high-rise building [3].

## **1.2 Motivation**

This study aims to analyze and investigate the influence of liquid tanks on the response of a seismic isolated structure. It can be achieved by considering a set of different partially filled liquid tanks with a variety of sizes and dimensions when the structure is subjected to a number of near-fault earthquake ground accelerations. A nonlinear response history analysis is conducted on a lead rubber bearing (LRB) isolated structure where a liquid tank is installed on the base of the structure, ultimately a comprehensive parametric study is performed on the response of the structure in terms of inter-story drift, bearing force, bearing displacement, and sloshing displacement of liquid tanks.

## **1.3 Literature Review**

This section has documented an overview of the research available in the literature, mainly concerned with the effect of liquid storage tanks on the seismic response of the base isolated structure.

T. Novo et al. studied Tuned Liquid Dampers for earthquake response control of buildings. The investigation focused on the performance of an isolated TLD under sinusoidal excitation at its base with various displacement amplitudes was studied by

finite element analysis method Sap2000 was used for finite analysis when the structure is subjected to dynamic force liquid sloshing induces unequilibrated impulsive loads in both sides of tank walls and these forces depend on the height of fluid inside the tank [4].

Thomas Furtmüller et al. studied the performance of a 3-story base excited small model of base-isolated shear frame structure equipped with TLCD. In this experiment, the standard dynamic test methods based on displacement and acceleration response measurement were used to determine the dynamic features of the shear frame and base isolation system separately in the base isolation subsystem. Viscous damping and friction effects were identified in this study. It can be concluded that the application of TLCD will lead to a 58% reduction in base displacement compared to a solely base-isolated structure [5].

Yongjian Chang, studied modified, tuned liquid damper (MTLD). This control system comprises of tuned liquid damper attached to the structure by four springs at four corners and two pivots at the centers of the rectangular tank to have both translation and rotations. He performed numerical and experimental investigations. He used Lu's model for numerical study and Real-time Hybrid Simulation (RTHS) for experimental research. The result is compared with the traditional TLD. It has been concluded that using the optimum value of  $L_s$  can be possible only for alpha and beta values that are less than 1 where the properly designed MTLCD is shown to be more effective than TLD. And finally, the preliminary design procedure of MTLCD is proposed for developing these devices [6].

Ali Ashasi-Sorkhabi et al. present the results of an extensive investigation to determine the dynamic response of TLD-structure systems. They use RTHS with various effective factors like mass, frequency, and structural damping ratios. A grid based FVM/FEM approach was used for numerical calculations. Experiments revealed that the TLD's structural performance improves by raising the mass ratio from 0.5% to 3%. However, for more than 3% mass ratios, the TLD effectiveness does not increase considerably, and in some instances, unexpected effects are detected [7].

Rafael O. Ruiz et al. proposed a new type of TLD, which includes a tuned liquid damper with a floating roof (TLD-FR). The finite element method was used to analyze the model. Different dynamic excitation was applied at the base of the rectangular base glass tank

supported by an ad hoc chassis. Two spherical joints attach to the floating roof made of polystyrene. The result shows that, despite the TLDs, the response of the TLD-FR is linear and behaves as a single degree of freedom system as a result of the floating roof, which prevents wave breaking. For practical designation of the device, they examine the relation between geometrical properties, the sloshing periods, and the efficiency index. find that the sloshing period depends only on length(L) for an aspect ratio( $R=H/L$ ) greater than 0.8, which means by keeping L constant and changing the water depth (H), you can modify fundamental sloshing periods. Also, it is observed that the efficiency index depends only on the aspect ratios [8].

In this study, Ali Pabarja et al. investigated the efficiency of tuned liquid dampers for suppressing the dynamic response of vertically irregular structures. The experimental investigation was done on a three-story one-bay steel structure with a height of 2.65m under free and forced vibration, where damping ratio, mode shapes, and natural frequencies were obtained. The conventional TLDs were placed on each floor separately, and the dynamic response for the structure with the TLD system was measured at each floor level. The maximum decrease of about 45% in displacement response of the structure-TLD system was observed when TLDs were tuned to the first and second natural frequencies, and both TLDs were placed on the structure's third floor. Similarly, the second configuration of the combined case also shows up to 40% mitigation of displacement response. Finally, a general conclusion is that a specific TLD with the same dimension would reveal different responses when installed on other floors [9].

Zili Zhang conducted a numerical and experimental study of the sloshing properties of sloped-bottom and flat-bottom tuned liquid dampers TLDs. The numerical investigation is performed by generalized eigenvalue problem (EVP) using classical potential theory and linear wave theory. The differential EVP is converted into an algebraic EVP by spatial discretization with a central difference approach; theoretical and numerical sloshing modes of the free surface elevation of flat-bottom TLD are in an excellent agreement where the odd-numbered mode shapes are asymmetric, which shows that the odd-numbered sloshing modes have more contributions to control force by TLD. However, for sloped-bottom TLD, no theoretical solutions exist. Experimental results validate the

numerical model after comparing the sloshing eigenfrequencies obtained from numerical outcomes, and the free vibration tests satisfactory agreement is achieved. It's found that the properties of sloshing modes are highly dependent on dampers' geometries. For a specific mean water level MWL, the eigenfrequencies of the flat-bottom TLD act as the upper limit of those of sloped-bottom TLDs for all possible angles and length ratios. The sloshing frequencies increase nonlinearly as MWL increases; when the slope angle and length ratio decrease, the sloshing eigenfrequency increases in a nonlinear manner [10].

Dhirendra K. Pandey, investigated TLD installed on a flexible pad which is similar to elastomeric bearing for base isolation called compliant TLD; the numerical analysis was performed by solving the equation of motion on a structure with a compliant TLD system, nonlinear sloshing, and wave breaking was obtained by applying Sun model the system is verified experimentally using white noise force vibration test, shake table and suite of ground motions on a three-storied scaled model of the frame structure. Finally, the difficulty of proper tuning in the conventional rigidly connected TLD has been eliminated by compliant TLD. The tuning, resonant sloshing, and wave breaking have been retained by applying this control device [11].

Zhu Fei et al. (2019) [12], carried out, a comparative investigation to determine the performance of TLD and TLCD using RTHS. They modeled a five-story reinforced concrete building on the computer and the Physical, models of TLD and TLCD were tested in the laboratory with the same premise of the same length, mass ratio, and structural parameters. The distributed real-time calculation system that is built-in MATLAB is used to solve the equations of motion. The result of both numerical and experimental studies indicated that both TLD and TLCD perform well in controlling the vibration; however, TLD is more effective than TLCD in energy dispersion when the liquid length, the mass ratio of both TLD and TLCD, and the structural parameters remain the same during testing. Hence, their result contradicts the finding of Bigdeli and Kim (2016).

Ji-Hwan Shin et al. studied a hybrid control strategy that uses tuned liquid damper TLD and active mass damper AMD to mitigate the structural vibration of a multi-story building. Developing this kind of system aims to combine the advantages of both TLD

and AMD. They claimed that TLD is in charge of suppressing the primary target mode, while AMD is in charge of suppressing the two peaks resulting from the application of TLD. Numerical simulation methodology was used to investigate the response of the structure. A building with 40 floors of 200m in height and 40m in width is numerically analyzed. They confirmed that sloshing modes other than the first sloshing don't affect the building vibration, which means that the SDOF model is sufficient for TLD to be analyzed. The experimental validation for this system was carried out on a single story with TLD and AMD mounted on the same floor. The numerical results are in good agreement with the experimental results [13].

K.P. McNamara et al. investigated the behavior of a single-degree structure-TLD system where the tank has a limited freeboard. The TLD is represented by the 2D incompressible smoothed particle hydrodynamics (SPH) model. The structure is modeled as an equivalent linear SDOF system through model analysis, and the validation for a sloshing tank with ceiling impact and SPH model is experimentally implemented. Their experiment simulates 63 structure-TLD systems to 4 hours of duration band-limited white noise excitation. They found out that the effectiveness of limited freeboard TLD in reducing structural motion was less than the unlimited freeboard TLD [14].

Emili Bhattacharjee et al. investigated the dynamic response of a structure with TLD when subjected to harmonic excitation. The harmonic force was applied to the shaking table on liquid tanks with different water depth and frequency ratios. This paper focused on a series of experimental tests on a scaled model of structure-tuned liquid damper systems with large-amplitude excitations because of the significant difference in the performance of large and small amplitude excitations. The effect of the water depth ratio is considered from 0.05 to 0.3. The result indicates that for each setup, optimum water depth exists that minimizes the response amplitude. Also, it was observed that the square TLD is less effective than rectangular TLD with different orientations. When they observed the frequency effect, they found that the structural response depends on the depth ratio for excitation frequency lower than the resonance frequency. However, near the resonance condition, the response amplitude suppresses considerably upon the attachments of TLD.

Similarly, no huge impact is observed when the excitation frequency becomes higher than the resonance frequency. Therefore, maximum response control is obtained when the structure is subjected to resonance at nearly 86.6% and 73.2% for different orientations of rectangular TLD. The effect of the tuning ratio on the structural response, which is the ratio of  $(F_w/F_s)$  in tuning the effectiveness of TLDs, has been found as 53.1% and 34.6% for different rectangular TLDs, which is acceptable for controlling the response of the structure [15].

Zhengyuan Tang et al. used a frequency domain analysis method for analyzing tuned liquid dampers installed on multi-degree freedom systems subjected to earthquake excitation. Generally, the frequency domain analysis method is limited for SDOFs systems; therefore, the substructure is decomposed into several smaller independent substructures, and the relationship between the overall structure and substructure is developed through the coordination conditions of force and displacement. For analyzing the damping performance of the TLD-installed MDOFs system in the frequency domain, they created a method for establishing the frequency domain transfer function of the TLD-MDOFs damping system by combining the concept of substructure and mod superposition. And this method has been verified by the RTHS experiment. There are two most important outcomes of this research [16].

- 1) Structures with a greater damping ratio performance are worse in damping effect, which indicates that TLD is not suitable for improving the seismic performance of the structure with a relatively high damping ratio, for example, damper-installed structures.
- 2) The comparison between the performance of the TLD-equipped structure designed by single-mode and multi-mode has been made. The result reveals that for the TLD with the same mass designed by the single-mode method, the multi-mode method performed significantly better in both acceleration and displacement response.

#### **1.4 Research Objectives and Aim of The Thesis**

The research work in this paper aims to analyze the effect of liquid storage tanks with different aspect ratios on the seismic response of base-isolated structures. The structure's

response will be computed based on the bearing force, bearing displacement, inter-story drift, and liquid sloshing displacement.

The objectives will be achieved by performing the following tasks:

- ❖ A literature assessment on the seismic response of liquid storage tanks on base-isolated buildings has been carried out to determine the most current advancements and significant research gaps in this topic.
- ❖ The conceptual and mathematical basis essential for modeling and analyzing seismic base isolation systems and liquid storage tanks will be addressed.
- ❖ With the support of the models existing in the literature, the numerical techniques employed in the parametric analysis will be developed and validated. The isolated model will be based on the isolated structure model presented by Dimitrios Konstantinidis [22]. And liquid storage tanks will be modeled based on the Housner spring-mass model presented by IITK guidelines for seismic design of liquid storage tanks.
- ❖ Within the scope of the thesis, a parametric study will be carried out on the structure's response to account for the influence of liquid storage tanks for different aspect ratios. In this study, the liquid tank will be examined by neglecting the tank wall flexibility and rigidly placed on the base floor of the building, partially filled with water, and considering water sloshing motion.
- ❖ The conclusion will be provided after an inclusive parametric study and the result and discussion, including recommendations for future investigations.

## **1.5 Overview of the Thesis Structure**

In this section, the structure of this thesis is discussed, which includes five chapters as follows:

In chapter one, a brief introduction to the base isolation system and liquid storage tanks is highlighted within the motivation section. In addition, the outcomes of the scientific

report are presented, along with the study's aims, and objectives are explained in the end structure of the thesis.

Chapter two, this chapter comprises four major sections that mainly consist of a detailed explanation of the seismic isolation system. The first section includes an overview, the second section working principles, and the third section types of the seismic isolation system are presented. The fourth section describes the design procedure for the lead rubber bearing isolator (LRB).

In chapter three, an overview of liquid storage tanks is mentioned, followed by an explanation of mechanical modeling of liquid storage tanks. Finally, design techniques for liquid storage tanks are addressed.

In chapter four, numerical modeling and analysis of two-dimensional seismic isolated structures with MATLAB script are explained as well as the selection of ground acceleration data required in the investigation.

Chapter five presents the parametric study of the structure's response, along with the discussion of the results.

Chapter six is the last chapter of this thesis work that contains the conclusion and recommendations for future studies.

## CHAPTER 2

### SEISMIC ISOLATION SYSTEMS

#### 2.1 Overview

Seismic base isolation has been deemed an efficacious earthquake resistance design strategy by applying a unique suspension system that decouples the super-structure from its substructure [17]. Decoupling is attained by increasing the horizontal flexibility of the system at the seismic isolation level [18].

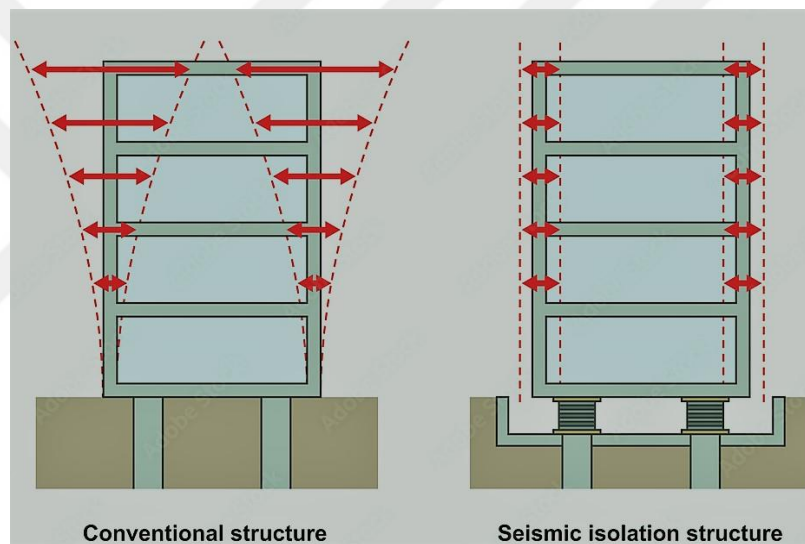


**Figure 2.1** Effect of Seismic Base Isolation [35].

#### 2.2 Working Principle of Seismic Isolation System

Seismic isolation is implemented with a laterally flexible and vertically almost rigid device, such as lead rubber bearings and frictional sliding elements placed between the foundation and the structure's base [5].

In this way, the fundamental period of the structure is shifted to a higher value, and if it's appropriately designed, the super-structure will almost behave like a rigid mass. Therefore, the deformation is concentrated in the bearings of the base isolation. The main disadvantage of the base-isolation system is significant dynamic displacement demands, which can be a limiting design factor. A passive hybrid control approach has been

suggested to overcome this limitation, comprised of base isolation and a tuned vibration absorber [5].

The figures (2.2 a, b) illustrate the elongation effect of the fundamental period of vibration, which results in the decline of lateral force and an increment in displacement responses [19].

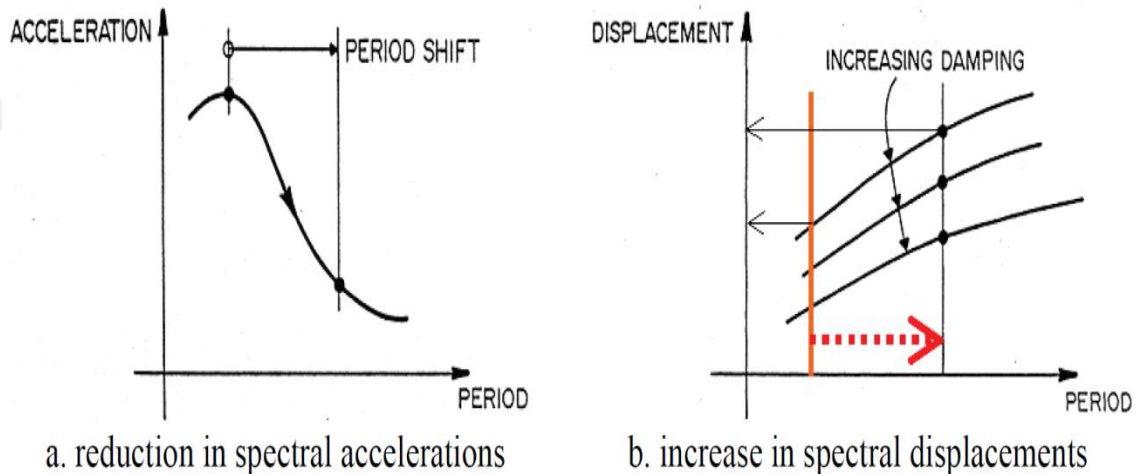


**Figure 2.2** Influence of Period Shift of Base Isolated Structure [19].

### 2.3 Types of Seismic Isolation

Generally, seismic isolation systems are categorized into two groups, namely elastomeric bearings, and sliding bearings.

Elastomeric bearings.

- ❖ Low-damping rubber bearings (natural or synthetic).
- ❖ High-damping natural rubber bearings (HDRB).
- ❖ Lead rubber bearings (LRB).

Sliding bearings.

- ❖ Flat sliding bearings.
- ❖ Spherical sliding bearings.

## **2.4 Sliding Bearings**

Friction is the basis for how a sliding isolator operates. This method is predicated on the idea that shear transmission reduces with reducing friction coefficient [36].

A sliding isolator utilizes two plates that slide over one another. These plates could be pure stainless-steel plates or a friction slider with a spherical surface. For sliding to begin, the amount of ground acceleration force should be more than the isolator's frictional force [37].

### **2.4.1 Flat Sliding**

The flat sliding isolator system generally works based on pure friction in which the two flat plates slide over one another; these plates are made up of stainless steel. When excitation occurs, the upper plate slides over the lower plate. Therefore, the superstructure behaves as a rigid body mass against earthquakes. The only criterion for an isolator to be operated is its oscillation force to be larger than its frictional force [37]. The fundamental benefit of this isolator is that the level of acceleration response is independent of the frequency and magnitude of the vibration, which suggests that these isolators can be applied to any site [36].

Beyond the benefits mentioned above, the flat sliding isolator has several drawbacks. The layout of the sliding surface is the primary issue. Since the sliding surface is indeed flat, there could be significant sliding and residual displacements. Lack of restoring force causes residual displacement [37]. A relatively high degree of friction coefficient is required to offer enough resistance and prevent unwanted displacement. However, a higher friction coefficient causes a higher external force demand for the isolator to slide [38]. As a result, the isolator maintains its non-sliding state during small seismic excitation values, and the building acts as a fixed base structure. As an outcome, the superstructure undergoes displacements and accelerations. These bearings are usually used with elastomeric isolators for self-centering.

### **2.4.2 Friction Pendulum System (FPS)**

The Friction Pendulum System is an improvement on the flat sliding system that addresses the primary issue with the flat sliding isolator's restoring force. FPS is modeled

on the well-established pendulum oscillation concept. Generally, this system is considered an excellent vibration control system that combines isolation, energy absorption, and restoring mechanisms [39]. The FPS has a movable component that serves as a slider and a spherical concave surface that serves as a foundation of the isolator. The contact surface between the slider and the base is made of a material called PTFE.

After the earthquake, the slider will return to its initial position because of the base plate's concavity under gravity. When there is a seismic vibration, the slider moves on the spherical surface, elevating the structure and absorbing energy through friction. As a result, it restores the building to its initial location and also lessens the residual displacement.

Besides all the advantages of FPS, the primary drawback of FPS is that its spherical sliding surface has a fixed period where it simply relies on the radius of curvature [37].

## **2.5 Elastomeric Isolators**

This type of isolator comprises a cluster of alternating steel shims and rubber layers. The steel shims provide vertical stiffness, while the rubber layers provide lateral flexibility. Additionally, the bearing has rubber covers on the top, bottom, and sides to protect the steel plates from corrosion [18].

### **2.5.1 Low Damping Rubber Bearings**

Low-damping rubber bearings are either natural or synthetic bearings. These bearings' lack to effectively dissipate energy results in small hysteresis loops, as shown in Figure 2.3 The damping ratios for low damping rubber bearing (LDRB) is between 2 to 3%, They are simple to build and model and their performance is not severely affected by factors such as loading history, temperature, or aging; however, they often require a supplemental damping system [20].

### **2.5.2 High Damping Rubber Bearings**

The dynamic characteristics of high damping rubber bearings' generally show high sensitivity to loading conditions; for instance, they are exposed to scragging, which is defined as a change in mechanical properties such as a decrease in stiffness and damping.

High-damping lead rubber bearings can dissipate large amounts of energy, resulting in larger hysteresis loops. They can provide 10 to 20% damping, and the damping properties can improve by adding "extra fine carbon black," oils, and resins. [20].

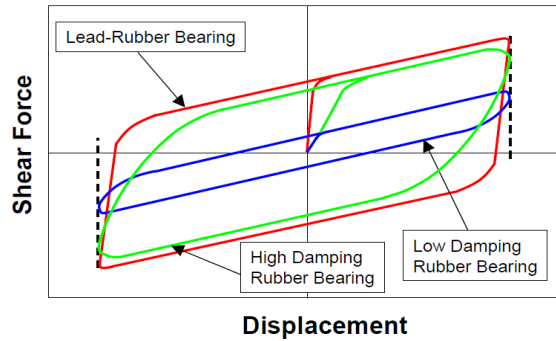


**Figure 2.3** Typical Hysteresis Loops for Elastomeric Bearings [36]

### 2.5.3 Lead Rubber Bearing Isolator

Lead-rubber bearing is an elastomeric isolator consisting of a central lead core, which contributes to enhancing the initial stiffness of the bearing and improving the energy dissipation capability of the bearing since it absorbs energy after the lead yields [20].

It was invented on April 1975 by W H Robinson, and soon after, the invention of lead rubber bearing was tested and used in the practical application of buildings and bridges. The primary reason for using a lead plug is that lead acts basically as an elastic-plastic solid and yields in shear at a comparatively low yield strength of 10 MPa [18]. In addition, lead has recrystallization and grain growth properties at room temperature and provides the required hysteretic damping. It's easily manufactured where an elastomeric bearing can be converted into a lead-rubber isolator by installing a lead core at its center. A hole is machined for the lead plug, or several holes can be made in rubber layers and steel shims. The lead is then forced into the hole or cast straight into it after machining into a plug. For the lead plug to lock with the steel plates and extend a bit into the rubber layers using either approach, it must be a tight fit in the hole [18].

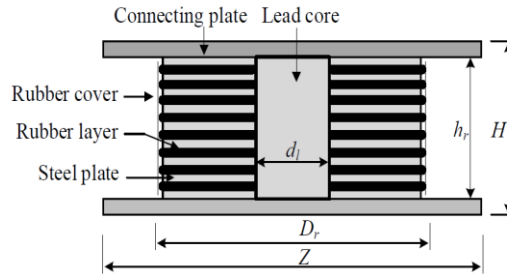


**Figure 2.4** Lead Rubber Bearing Isolator [21].

### 2.5.4 Properties of Lead Rubber Bearing Isolator

In order to obtain the force-displacement loops of lead-rubber isolators at the time of horizontal displacements of design earthquakes and severe earthquakes, test techniques were developed at seismic velocities when an axial load simulating the weight of the structure was applied to confirm that the temperature rises and strain rates of lead would be the same during simulated earthquakes. The hysteresis loops of the elastomeric bearing are generally elastic with a small amount of hysteresis, while lead rubber bearing acts as a plastic-solid and increases the shear force capacity of bearing by roughly 235kN according to W. H. Robinson experiment compared to only elastomeric bearing [18].

Generally, Lead Rubber Bearing isolation can be defined and modeled as bilinear based on four primary parameters, including (1) characteristic strength  $Q$ , (2) post-yield stiffness  $K_2$ , (3) maximum displacement  $D_{max}$  (4) yield-displacement  $D_y$  as described in Figure 2.5 [21]. These parameters will be discussed in chapter 4 on isolator modeling.

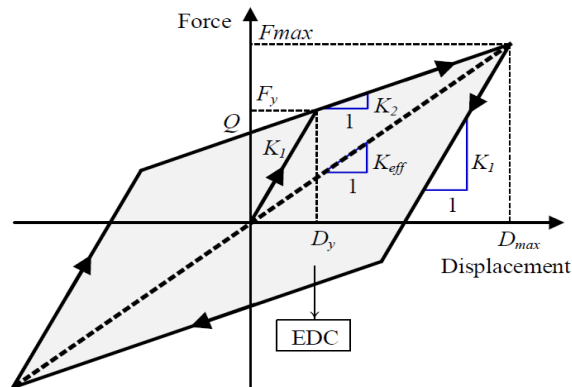


**Figure 2.5** Force Displacement Hysteresis Loop of Lead Rubber Bearing [21].

## 2.6 Modeling and Parameters of Lead Rubber Bearing

This study has carried out a comprehensive set of nonlinear dynamic analyses on a Lead Rubber Bearing isolation. This study's mechanical modeling and design procedure were adopted based on the study presented by Dimitrios Konstantindis (2015) [22], who utilized the Bouc-Wen model, which has been used widely by many researchers to get hysteretic loops.

The isolator parameters to be used in the Bouc-Wen model such as pre-yield stiffness, post-yield stiffness, yield strength, etc. can be obtained through experiments. The isolator manufacture will provide either loops or the parameters  $(U_y, \alpha, K_2)$  or  $(U_2, K_e, K_2)$ , which will define a purely bilinear model. In this paper, a six-parameter model was considered.

The restoring force of isolated bearing is defined by equation (2.1) as shown in Figure (2.6),  $\alpha$  is defined as the ratio of post-yield stiffness to the elastic stiffness  $K_e$ ,  $u_{(t)}$  shows the Displacement,  $U_y$  represents the yield displacement,  $Z_{(t)}$  indicate the dimensionless variable the other three parameters generally controls the rounded shape of the loops and has defined in the  $Z_{(t)}$  equation [2.2].

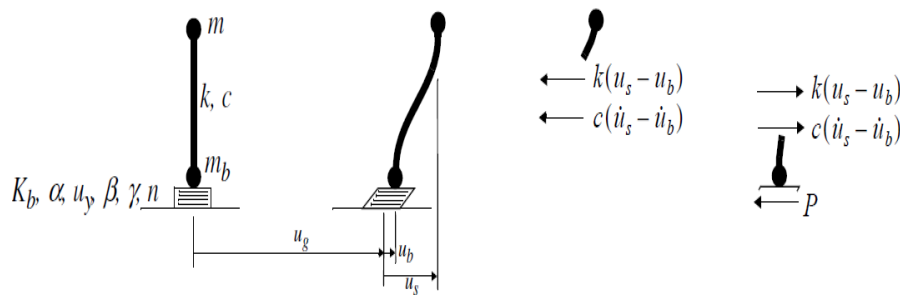


**Figure 2.6** Restoring Force of Isolated Bearing [22]

$$p_{(t)} = \alpha K_c u_{(t)} + (1 - \alpha) K_e u_y Z_{(t)} \dots \dots \dots (2.1)$$

the restoring force from equation (2.1) contains  $Z_{(t)}$ , a term that requires be defined  $Z_{(t)}$  as a dimensionless first order differential equation. It will be given by equation (2.2), in that equation  $n$  controls the sharpness of the curve, which shows the state of transition from elastic to inelastic.  $\gamma$  and  $\beta$  are the parameters that control the shape of the loops.

$$u_y \dot{z}(t) + \gamma |\dot{u}(t)| z(t) |z(t)|^{n-1} + \beta |\dot{u}(t)| z(t)^n - \dot{u}(t) = 0 \dots \dots \dots (2.2)$$

Q is the bearing's characteristic strength, dependent on many factors such as lead area (A<sub>L</sub>) and effective yield stress of lead (σ<sub>YL</sub>).

$$Q = A_{(L)} \times \sigma_{YL} \text{ (MPa)} \dots \dots \dots (2.3)$$

M<sub>Pa</sub> indicates the unit as mega pascal

K<sub>d</sub> represents post elastic stiffness which depends on three factors G, the shear modulus of rubber, A bonded area of rubber A, and the total rubber thickness T<sub>r</sub>.

$$K_d = \frac{GA_r}{T_r} \dots \dots \dots (2.4)$$

α is the post-yield elastic stiffness ratio to the pre-yield elastic stiffness.

$$\alpha = \frac{K_d}{K_1} = 0.1 \dots \dots \dots (2.5)$$

D<sub>y</sub> is the yield displacement related to the characteristic strength of the bearing.

$$D_y = Q / (K_1 - K_d) \dots \dots \dots (2.6)$$

f<sub>y</sub> is the yield force of lead rubber bearing, where K<sub>1</sub> represents the initial stiffness.

$$f_y = K_1 * D_y \dots \dots \dots (2.7)$$

K<sub>eff</sub> the effective bearing stiffness is denoted by K<sub>eff</sub>

$$K_{eff} = K_1 \frac{Q}{D_y} \dots \dots \dots (2.8)$$

## CHAPTER 3

# LIQUID STORAGE TANKS SUBJECTED TO HORIZONTAL EARTHQUAKE BASE EXCITATION

### 3.1 Overview

This section presents a general overview of liquid storage tanks subjected to earthquake excitations. The Liquid tanks are crucial structures and are widely used in industry and nuclear power plants [24]. Typically, buildings have storage water tanks built for the services. These utility storage tanks can also be used to control the building system's response since it has been noted that the sloshing of liquid stored in containers may function as a structural seismic control mechanism [3].

The liquid tanks can be constructed in different shapes, such as rectangular, square, and cylindrical. Cylindrical tanks are most frequently employed due to their ease of design and building and their superior resistance to hydrostatic and hydrodynamic loads [25]. Water tanks are typically constructed on tower supports (made of steel or reinforced concrete) to provide the necessary pressure and prevent the need for pumping facilities. Water tanks in the seismic zone must still be functional after earthquakes to provide enough water for firefighting purposes [25].

Due to the interaction between the liquid and the structure, the seismic behavior of the liquid storage tank is quite complex, making the design process difficult from a seismic design perspective. In the last few decades, researchers have presented numerous techniques to model the structural seismic response of liquid storage tanks, such as the test analysis method, the distributed mass method, and the concentrated mass method [24]. Tanks can be modeled as rigid or flexible tanks depending on the thickness of their walls. Lumped mass models for rigid fluid tanks were proposed by Housner [27]. Rosenblueth, and Newmark [43].

### 3.2 Fundamentals of Liquid Sloshing

Sloshing refers to the movement of liquid in a partially filled tank due to externally applied forces [27]. When an earthquake occurs, the content of a ground-supported liquid

tank will experience a sloshing motion. If a tank or reservoir containing water and having a "free surface" is subjected to horizontal seismic ground motion, both the tank wall and the water inside undergo horizontal acceleration; as a result of the ground acceleration, the water in the tank's lower section acts as a mass that is almost rigidly attached to the tank wall. This mass, which is referred to as an "impulsive liquid mass," accelerates alongside the tank wall and exerts an "impulsive hydrodynamic pressure" on the tank wall and base. Similarly, the "liquid mass" in the tank's upper portion undergoes sloshing. This mass is known as "convective liquid mass," and it applies "convective hydrodynamic pressure" on the tank wall and base [27].

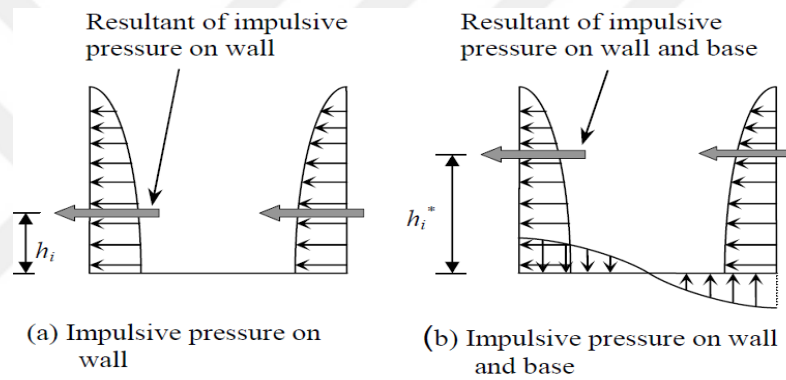


**Figure 3.1** Distribution of impulsive hydrodynamic pressures [27].

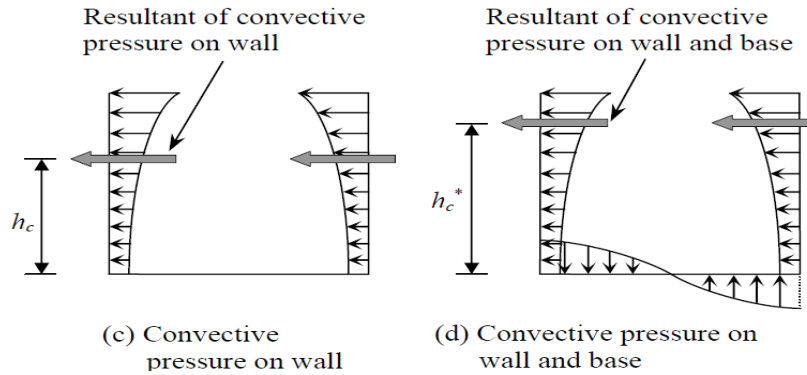


**Figure 3.2** Distribution of convective hydrodynamic pressures [27].

### 3.3 Mechanical Modeling of Liquid Storage Tanks

The modeling procedure for the liquid storage tank to be used in this study will be described in this section. This procedure will be used in MATLAB scripts for analysis to

determine the sloshing impact of liquid storage tanks over the seismic structure response [33].

Three cases that include eleven liquid storage tanks made of reinforced concrete were considered. The shapes of the tanks are rectangular. Each tank has a different size and capacity to account for a wide range of aspect ratios, such as depth to height and length to depth ratios, and they are placed on the bass floor of the structure.

Researchers have conducted in-depth studies to analyze the damages caused due to earthquake motions on liquid storage tanks and proposed techniques and design procedures to determine internal and external forces exerted on tank walls. Housner was the first who develop the spring-mass model by considering hydrodynamic pressure distribution in rigid tanks [27]. Later, Veletsos A.S included the influence resulting from shell elasticity in the model [40]. Recently Praveen K. Malhotra and Michael Meekins [28]. analyzed the seismic response of horizontal tanks. Their findings result that only about 28% of the liquid flows with the tank wall and produces seismic forces in the longitudinal direction, according to the fluid-structure interaction in the tank. The other 72% of the liquid sloshes close to the free surface and produces negligible seismic forces [28].

It has been observed that the sloshing of liquid in a liquid storage tank will help control the buildings' seismic response [3]. A simple model which accounts for the sloshing motion of liquid in a rigid storage tank was presented by (Housner 1957).

Two cases of liquid tanks that will be considered in this study were modeled based on Housner's (1963a) model, while the formula for calculating the design parameters is followed as per IITK-GSDMA guidelines [33].

The following assumptions will be considered in modeling liquid storage tanks for this study:

- ❖ The liquid was considered incompressible irrotational, and homogeneous.
- ❖ The walls of the tank were considered rigid, and the deformation of tank walls was neglected.
- ❖ The pressure on the free surface of the liquid before ground excitation is regarded as constant.

❖ Unit weight of water is counted as  $1000\text{kg}/\text{m}^3$ .

Figure 3.2 shows the parameters, which will be explained in the later sections.  $h_i$  is the height at which the resultant impulsive hydrodynamic pressure on the wall is placed.

$h_i^*$  is the height at which the resultant impulsive hydrodynamic pressure on the wall and base is situated. If the impact of base pressure is ignored, the impulsive mass of fluid  $m_i$  will act at a height  $h_i$ , and if the effect of base pressure is considered, then  $m_i$  will locate at the height of  $h_i^*$ . Accordingly,  $h_c$  is the height from the bottom of the container wall at which the resultant convective pressure on the wall is situated, while  $h_c^*$  denotes the height at which the "convective pressure" acts on the wall [29].

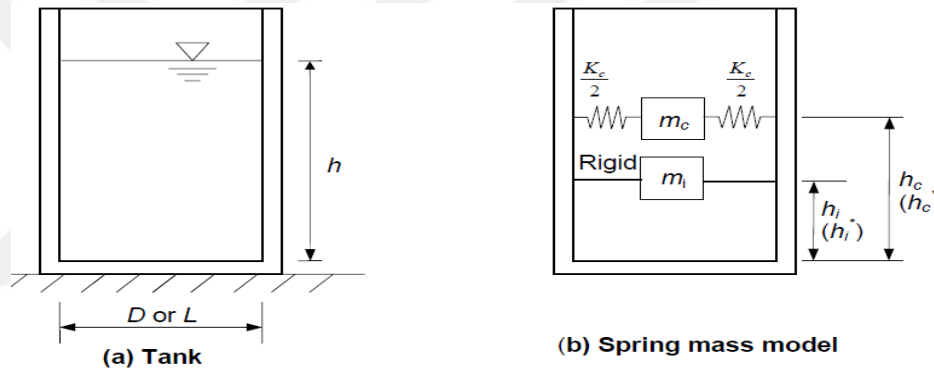


**Figure 3.3** Spring Mass Model for Circular and Rectangular Tanks [29].

Steps to obtain design parameters of liquid storage tanks:

1): once the dimensions (length L, height h) and the shape of the tank are decided next step is to compute total liquid mass (m) and empty tank mass  $m_t$  then, the whole designed parameters can be obtained through equation (1-8).

$$m = \rho \times v \times g \dots \dots \dots (3.1)$$

$\rho$ - is the density of water which is  $1000\text{Kg}/\text{m}^3$ .

$g$ - is gravitational constant  $9.81\text{m}/\text{s}^2$ .

$v$ - is the volume of water.

$h$ - is the height of the water inside the tanks.

$L$ - is the length of rectangular storage tanks, which is taken from Table 3.1

Convective mass  $m_c$  can be acquired from equation (1)

$$\frac{m_c}{m} = 0.264 \frac{\tanh(3.16 \frac{h}{L})}{\frac{h}{L}} \dots \dots \dots (3.2)$$

Impulsive mass  $m_i$  will be calculated using (2) after casting values for the length of the tank and  $h$  height of the water inside the tank

$$\frac{m_i}{m} = \frac{\tanh(0.866 \frac{L}{h})}{0.866 \frac{L}{h}} \dots \dots \dots (3.3)$$

$h_c$  height at which the resultant convective hydrodynamic pressure acts will be calculated by relation (3).

$$\frac{h_c}{h} = 1 - \frac{\cosh(3.16 \frac{h}{L}) - 1}{3.16 \frac{h}{L} \sinh(3.16 \frac{h}{L})} \dots \dots \dots (3.4)$$

Convective mass is attached to the tank's wall by stiffness  $K_c$  which will be obtained by relation (4).

$$K_c = 0.833 \frac{mg}{h} \tanh^2(3.16 \frac{h}{L}) \dots \dots \dots (3.5)$$

The damping coefficient of water in liquid storage tanks can be calculated from the following relation after getting values for  $m_c$  and  $K_c$ .

$$C_c = 0.005 \times 2 \sqrt{K_c \times m_c} \dots \dots \dots (3.6)$$

These parameters will be cast into the dynamic equations of motion, and a MATLAB script will be generated to analyze the seismic isolated structure.

In this part, three sets of liquid storage tanks are explained, and mechanical parameters for each tank are presented in Tables (3.1,3.2,3.3).

### 3.3.1 Mechanical Analogue for Tanks Case One

The first case includes five small rectangular liquid storage tanks represented by LT1, LT2, LT3, LT4, and LT5. Each has different length-to-height ratios in order to account for various aspect ratios.

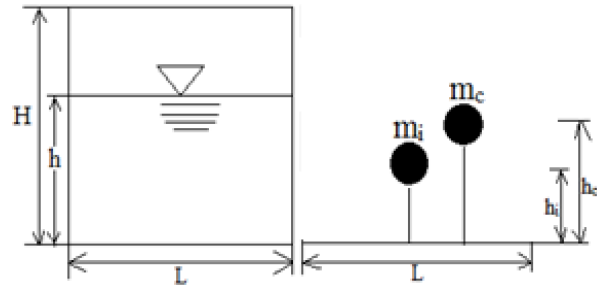


**Figure 3.4** Mechanical Analogue of Liquid Tank Case One

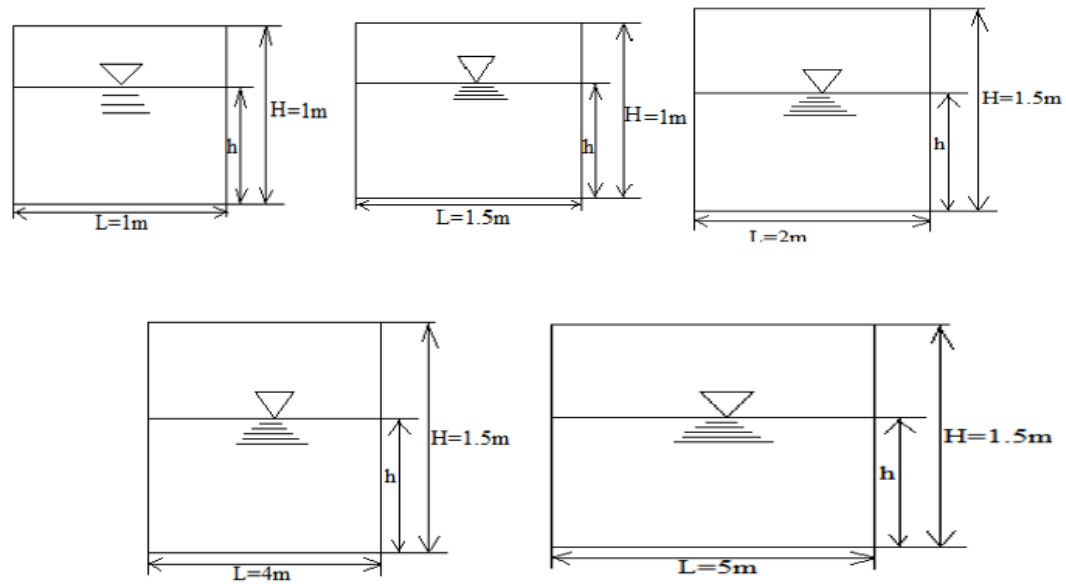


**Figure 3.5** Liquid Tanks LT1, LT2, LT3, LT4, LT5

**Table 3.1** Model Parameters of Liquid Storage Tanks

S. No	L (m)	h (m)	B (m)	H (m)	h/L	Water mass (tons)	$m_t$ (kN)	$m_c$ (kN)	$m_i$ (kN)	$K_c$ (kN/m)	$m_b$ (kN)
<b>LT1</b>	1	0.5	0.5	1	0.5	0.25	17.5	1.189	1.13	33.8	102.8
<b>LT2</b>	1.5	0.5	0.5	1	0.3	0.375	23.75	2.28	1.19	47.082	109
<b>LT3</b>	2	1	1	1.5	0.5	2	55	9.4	10.59	135.29	149.8
<b>LT4</b>	4	1	2	1.5	0.25	8	130	54.56	22.6	278.0	236.8
<b>LT5</b>	5	1	2	1.5	0.2	10	155	72.4	22.6	250.8	261.8

### 3.3.2 Mechanical Analogue of Liquid Tanks Case Two

Case two comprises of six large liquid tanks with two different mechanical analogues in which the first three liquid tanks (LT6, LT7, and LT8) are considered as sloshing liquid tanks. All have equal sizes but contain different water depths. It was modeled based on the spring-mass model presented by Housner [33]. The model is shown in Figure 3.6

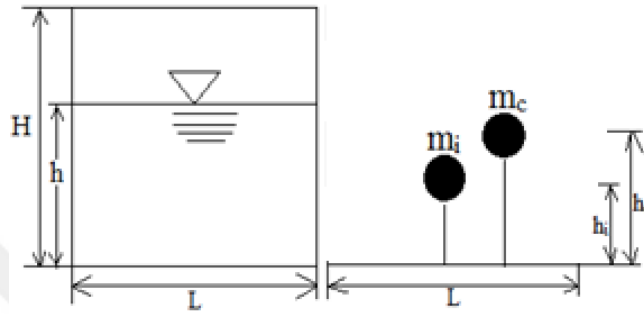


**Figure 3.6** Mechanical Analogue of Liquid Tank case two

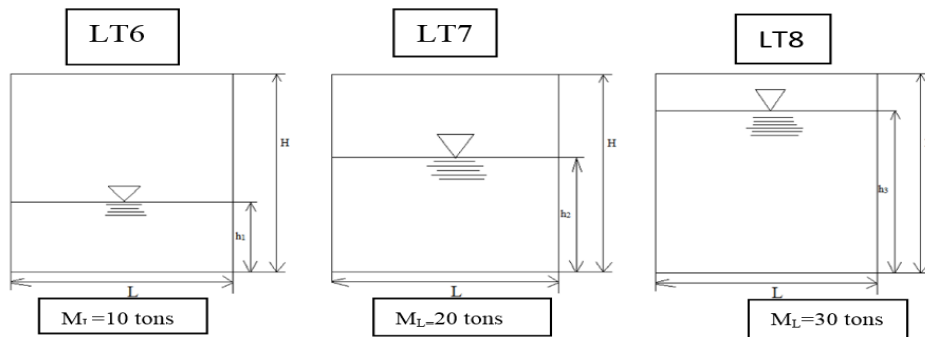


**Figure 3.7** Liquid Tanks case two.

$$\frac{h_1}{L} = 0.25 \quad \text{height to length ratio of LT6} \quad h_1 = 1 \text{ m}$$

$$\frac{h_2}{L} = 0.5 \quad \text{height to length ratio of LT7} \quad h_2 = 2 \text{ m}$$

$$\frac{h_3}{L} = 0.745 \quad \text{height to length ratio of LT8} \quad h_3 = 3 \text{ m}$$

**Table 3.2** Model Parameters of Liquid Storage Tanks for First Option

S. No	H (m)	L (m)	B (m)	$h_w$ (m)	Water mass (Tons)	$m_t$ (kN)	Floor mass (kN)	$m_i$ (kN)	$m_c$ (kN)	$K_c$ (kN/m)	Damping $C_c$ (kN.S/m)
LT6	3.5	4	2.5	1	10	138.7	84.2	28.2	68.2	347.5	1.5
LT7	3.5	4	2.5	2	20	138.7	84.2	106.4	95.16	736.3	2.6
LT8	3.5	4	2.5	3	30	138.7	84.2	208.8	101.7	787.7	2.8

### 3.3.3 Mechanical Analogue of Liquid Tanks Case two

The last three liquid tanks (LT6R, LT7R, and LT8R) are assumed to have rigid liquid mass the figure 3.8 shows the mechanical analogue of these tanks.

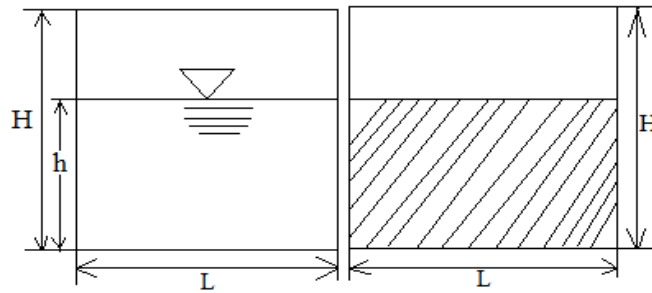


**Figure 3.8** Mechanical Analogue of Liquid Tanks case 2

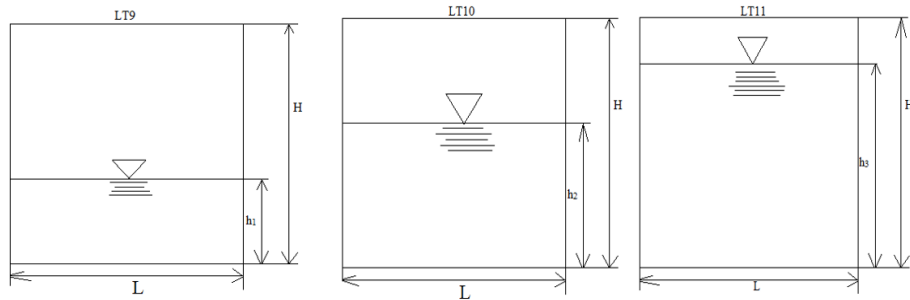


**Figure 3.9** Liquid Tanks for Case Two

$$\frac{h_1}{L}=0.25 \quad \text{height to length ratio of LT9} \quad L=4\text{m} \quad h_1=1\text{m}$$

$$\frac{h_2}{L}=0.5 \quad \text{height to length ratio of LT10} \quad L=4\text{m} \quad h_2=2\text{m}$$

$$\frac{h_3}{L}=0.745 \quad \text{height to length ratio of LT11} \quad L=4\text{m} \quad h_3=3\text{m}$$

**Table 3.3** Parameters of Liquid Storage Tanks

<b>Liquid Tanks</b>	<b>L (m)</b>	<b>B (m)</b>	<b>h<sub>w</sub> (m)</b>	<b>H (m)</b>	<b>Mass of Water (Tons)</b>	<b>m<sub>t</sub> (kN)</b>	<b>Floor mass (kN)</b>
<b>LT6R</b>	4	2.5	1	3.5	10	138.75	84.25
<b>LT7R</b>	4	2.5	2	3.5	20	138.75	84.25
<b>LT8R</b>	4	2.5	3	3.5	30	138.75	84.25

## CHAPTER 4

### NUMERICAL STUDY

This chapter is dedicated to the modeling of base-isolated structures as well as analysis procedure for structures with installed liquid storage tanks. The base-isolated structural model used in this study was adapted from the study of Konstantinidis [20]. First, the parameters of the model will be calculated. Afterward, the equations of motion will be generated. Finally, the model will be used for the analysis of the seismic response of the base-isolated structure when the liquid storage tank is placed on the base floor. In this study, Lead Rubber Bearings are used as seismic isolators.

The following topics will be discussed in this section:

- ❖ A brief description of seismic base isolated frame
- ❖ Governing equations of motion
- ❖ Selection of ground acceleration records
- ❖ Comparison of results to check the model

#### 4.1 Description of the Isolated Structure

The model setup used in this study is described in this section. It presents a single-bay single-story rubber base-isolated structure with a rectangular tank partially filled with water. The tank is rigidly installed on the base floor; Figure 4.1 shows the schematic diagram of a base-isolated structure with a rectangular storage tank. The column and slab dimensions are (0.4×0.4) m and (3× 5 × 0.15)m, respectively. The structure is modeled as a 2D frame with a rigid diaphragm for the top and base slabs; therefore, the lumped masses provide SDOFs with  $m=84.25\text{KN}$ , the natural frequency of the structure  $\omega_n=33.54\text{rad/sec}$ , and the fundamental period of 0.18 seconds with ( $\xi=10\%$ ) damping ratio.

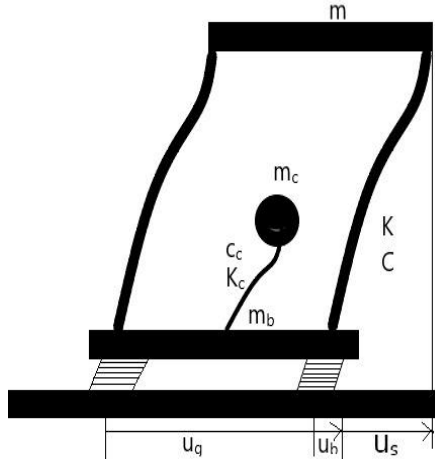


**Figure 4.1** Schematics Model of Isolated Structure with Liquid Tank

## 4.2 Analysis of the Model and Governing Equations of Motions

In this section, the equations of motion and the procedure to analyze the model will be discussed. The model in this study includes a base-isolated structure and liquid storage tanks. The base-isolated structure model was present in literature by Konstantinidis [20], where the necessary check will be performed based on that. However, the computation of parameters for the liquid storage tanks is based on the Housner spring-mass model, and the steps and formulations were followed according to the guidelines presented by IITK [33].

The mechanical model and the parameters for the liquid tanks and isolation system were discussed in the previous chapters. The following governing equations of motion are derived considering a Lead Rubber Bearing isolator and a rectangular liquid tank with various aspect ratios.

The structure is a 2D shear frame single story with a plan dimension of 5m×3m length along the x-axis and y-axis, respectively, and a height of 3.5m of each column. The column's cross-sectional area is provided as (0.4×0.4) m, 120mm thickness of the slab is considered for the base and top floors. The top floor weight is 84.25KN, and the total weight of the structure, including the weight of the base floor, is 185.95KN. The moment of inertia of each column  $I=2.133 \times 10^{-3} \text{ m}^4$ . The grade of concrete is assumed to be C25;

accordingly, the characteristic strength of reinforced concrete is determined by  $E_{cg}=5000\sqrt{f_{ck}}$  MPa. A rigid diaphragm is applied, and the structure's mass is considered to lump at floor level. Therefore, each floor only has a translation degree of freedom in the unidirectional global X-axis in the analysis. In this respect, we only consider the horizontal component of ground acceleration.

In the following governing equations of motion

$m$  is the structural mass

$\ddot{u}_s$  is the structural acceleration

$c$  is damping coefficient

$\dot{u}_s$  is the structural velocity

$\dot{u}_b$  is the bearing velocity

$k$  is the stiffness of the structure

$u_s$  is the structural displacement

$u_b$  is bearing displacement

$\ddot{u}_g$  is the ground acceleration record in units of  $g$

The second equation is concerned with the sloshing portion of the liquid mass. Water is used for the liquid inside the tank. The  $m_c$ ,  $c_c$ ,  $k_c$ , and  $u_c$  are the convective mass, damping constant, stiffness, and displacement, respectively. The third mass is the base floor mass, where the base slab is fixed on the isolator (P), representing the restoring force of the isolation system from the relation (2.1).[22]

$$m\ddot{u}_s + c(\dot{u}_s - \dot{u}_b) + k(u_s - u_b) = -m\ddot{u}_g \dots \dots \dots (4.1)$$

$$m_c\ddot{u}_c + c_c(\dot{u}_c - \dot{u}_b) + k_c(u_c - u_b) = -m_c\ddot{u}_g \dots \dots \dots (4.2)$$

$$m_b\ddot{u}_b - c(\dot{u}_s - \dot{u}_b) - c_c(\dot{u}_c - \dot{u}_b) - k(u_s - u_b) - k_c(u_c - u_b) + p = -m_b\ddot{u}_g \dots \dots \dots (4.3)$$

Since the MATLAB program was used in this study to perform dynamic analysis, writing a script is required to make it solvable for MATLAB. The equations of motion must be written in a state-space format in order to solve them with MATLAB ODE solvers.

The procedure to solve state-space equations of motion in MATLAB.[22]

- Writing .m script file.
- Define the model parameters such as masses, damping ratios, stiffnesses, etc.
- Load the ground acceleration record containing seismic events' acceleration, displacement, and velocity-time history.
- Using one of these built-in solvers (ODE15, ODE23, ODE45, etc.). Solve the equations of motion.

$$Y(t)=(y_1 \ y_2 \ y_3 \ y_4 \ y_5 \ y_6 \ y_7)^T=(u_b \ \dot{u}_b \ u_s \ \dot{u}_s \ u_c \ \dot{u}_c \ z)^T$$

$$Y \cdot (t) = \begin{bmatrix} \dot{y}_1 \\ \dot{y}_2 \\ \dot{y}_3 \\ \dot{y}_4 \\ \dot{y}_5 \\ \dot{y}_6 \\ \dot{y}_7 \end{bmatrix} = \begin{bmatrix} \ddot{u}_b \\ \ddot{u}_b \\ \dot{u}_s \\ \ddot{u}_s \\ \dot{u}_c \\ \ddot{u}_c \\ \dot{z} \end{bmatrix}$$

$$\begin{bmatrix} y_2 \\ -1/m_b(\alpha \times k_e \times y_1 + (1-\alpha)k_e \times u_y \times y_7 - C(y_4 - y_2) - C_c(y_6 - y_2) - k(y_5 - y_1) - K_c(y_5 - y_1) - \ddot{u}_g) \\ y_4 \\ -1/m(C(y_4 - y_2) + K(y_3 - y_1) - \ddot{u}_g) \\ y_6 \\ -1/m_c(C_c(y_6 - y_2) + k_c(y_5 - y_1) - \ddot{u}_g) \\ -1/u_y(\gamma|y_2||y_7|^{n-1} + \beta \times y_2|y_7|^n - y_2) \end{bmatrix} \dots\dots(4.4)$$

Equation (4.4) represents the state space formulation where this equation must be written as a function to be called by the ODE45 solver to perform the dynamic analysis by MATLAB.

### 4.3 Selection of the Ground Motion Records

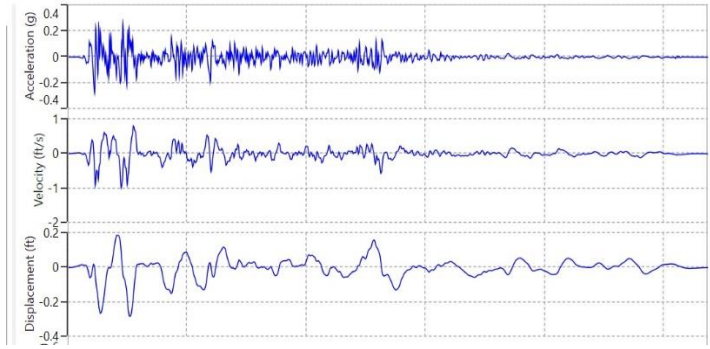
The process of selecting and modifying appropriate records is critical. In nonlinear dynamic analysis, a proper selection and modification of ground motion used in the study can yield a response with minimal divergence. This study used six near-fault earthquakes uni-directionally to the base of a seismically isolated structure. These records were obtained from the Strong Ground Motion database of the Pacific Earthquake Engineering Research (PEER) [31]. Near-fault sites are those within 9.3 miles (15km) of the surface projection of faults capable of generating seismic events of magnitude seven or larger and within 6.2 miles (10km) of causing earthquakes with a magnitude of 6 or higher according to ASCE 7-22 [30]. The nature of a near-fault earthquake is pulse-like with large PGV and PGD.

Table 4.1 shows six near-fault ground accelerations that will be loaded into MATLAB as input data. Some of the critical parameters of each event are described.

**Table 4.1** Lists of Features of Six Near-Fault Ground Excitation

No	Earthquake Name	RSN	Date	Time Step(s)	Magnitude	PGA (g)	PGV (cm/s)	PGD (cm)	Predominant period (s)	Housner intensity (cm)
1	Imperial Valley-2	6	1940	0.01	6.95	0.28	30.95	8.76	0.46	129
2	Kocaeli Turkey	1165	1999	0.005	7.51	0.23	76.68	96.6	0.28	105
3	Cape Mendocino	3750	1992	0.005	7.01	0.26	71	135	0.34	128
4	Northridge-01	1086	1994	0.02	6.69	0.6	77	16	0.52	261
5	Chi-Chi	1504	1999	0.005	7.62	0.49	920	10123	3.48	337
6	Iwate	5663	2008	0.01	6.9	0.69	40	20	0.18	146

The graphs in the following section are the acceleration time history of those earthquakes which will be used as input ground acceleration in the analysis. The PGA range of (0.23-.69) from the PEER database [32]. The data was loaded in MATLAB, where the given graphs were manipulated for response history analysis.



**Figure 4.2** Ground Acceleration Time History Centro Array #9

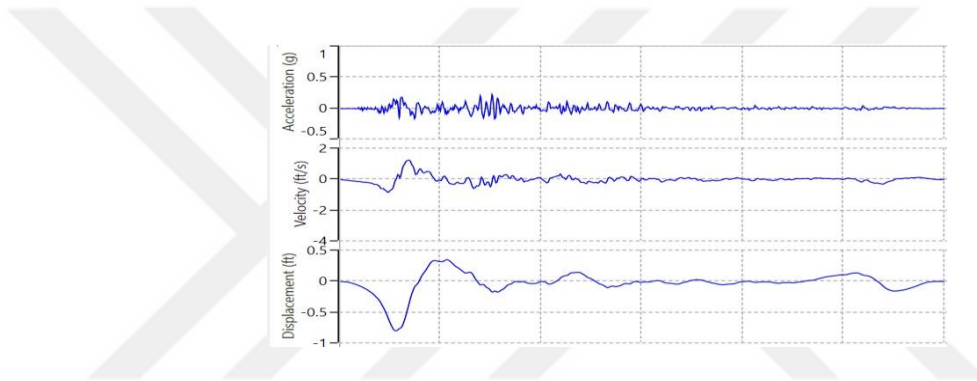


**Figure 4.3** Ground Acceleration Time History of Izmit,90

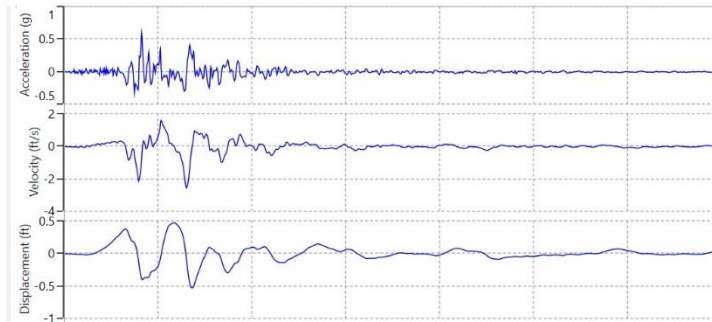


**Figure 4.4** Ground Acceleration Time History of Northridge-01 Med Ff, 90

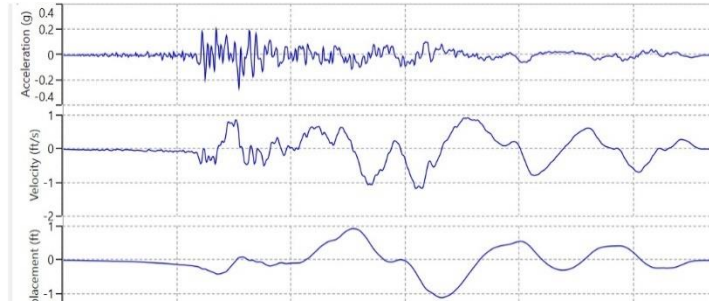


**Figure 4.5** Ground Acceleration Time History of Cape Mendocino, 270

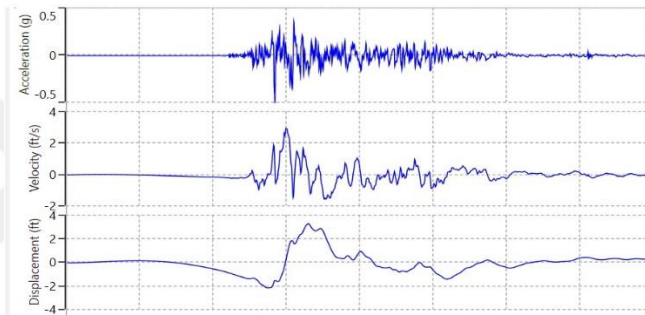


**Figure 4.6** Ground Acceleration Time History of Chi-Chi, Tcu067, EW

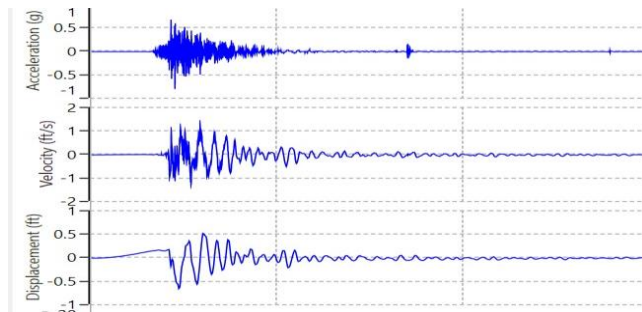


**Figure 4.7** Ground Acceleration Time History of Iwate, Myg004, EW

## CHAPTER 5

### RESULTS AND DISCUSSION

#### 5.1 Results and Discussion

In this chapter, various analysis factors are described in detail for three cases of this research study. The response of the seismic base-isolated structure with the rectangular liquid tank is described under six near-fault earthquakes. The features of the responses which will be acquired and analyzed in the following sections include bearing force, bearing displacement, story drift, and the sloshing height of the liquid.

##### 5.1.1 Liquid Tank Case One

Liquid tanks (LT1, LT2, LT3, LT4, and LT5) are small rectangular liquid tanks with different height to length ( $h/L$ ) ratios. The dimensions and the mechanical analogue system properties of each tank is listed on Table 3.1. Here, the structure performance for individual liquid tanks is evaluated for different earthquake records presented in Chapter 3. Based on bearing force, displacement, and story drift, the result will be discussed.

##### 5.1.2 Bearing Force

Bearing force for an isolated building is an important aspect, and it depends on various factors such as ground acceleration, types of isolation, the weight of the super-structure, etc.

In this part, the effect of liquid tanks on the bearing force of an isolated building is investigated for six near-fault earthquake events. It was observed that with increasing the sizes of the fluid tanks, the bearing force of the isolated building under four earthquakes named as Kocaeli, Cape Mendocino, Chi-Chi, Iwate, illustrate the increase of 35%, 114%, 124%, 39%, respectively. However, Imperial Valley-02 and Northridge-01 demonstrate a decrease of 35% and 18% bearing force, respectively, as shown in Figure 5.1

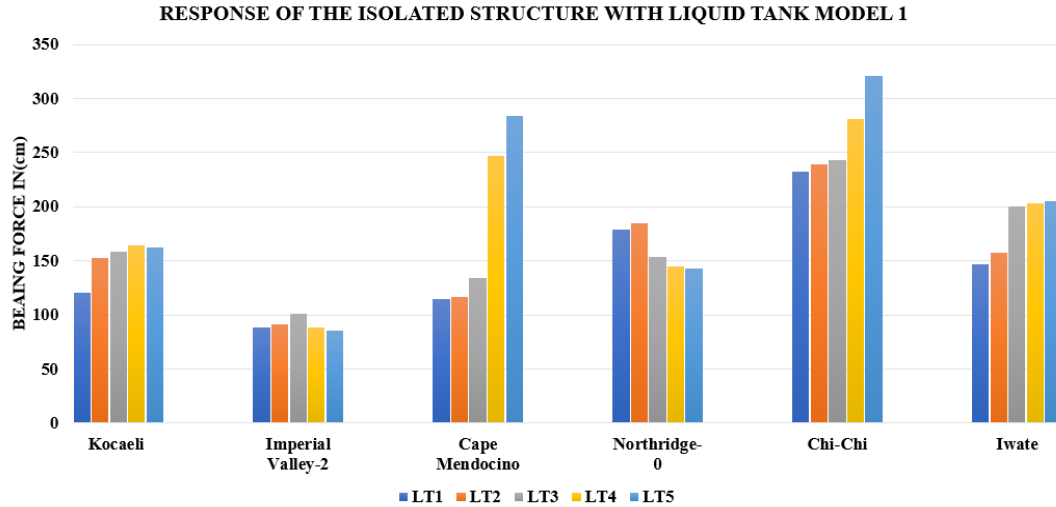


**Figure 5.1** Response of Isolated Building with Liquid Tanks

### 5.1.3 Bearing Displacement

for isolated structures bearing displacement, demand is high, which would be a design challenge. Here the displacement response of the base-isolated building will be discussed for the liquid tanks case one.

The bearing displacement increases with increasing the sizes of liquid tanks from LT1 to LT5 in the same way as the bearing force has shown an increase; the bearing displacement also indicates a rise under four earthquakes such as Kocaeli, Cape Mendocino, Chi-Chi, and Iwate which is 55%, 235%, 45%, 56% respectively. On the contrary, the two records, Imperial valley-02 and Northridge-01, show a decrease in bearing displacements of about 5.5% and 27%, respectively, which is explained in Figure 5.2.

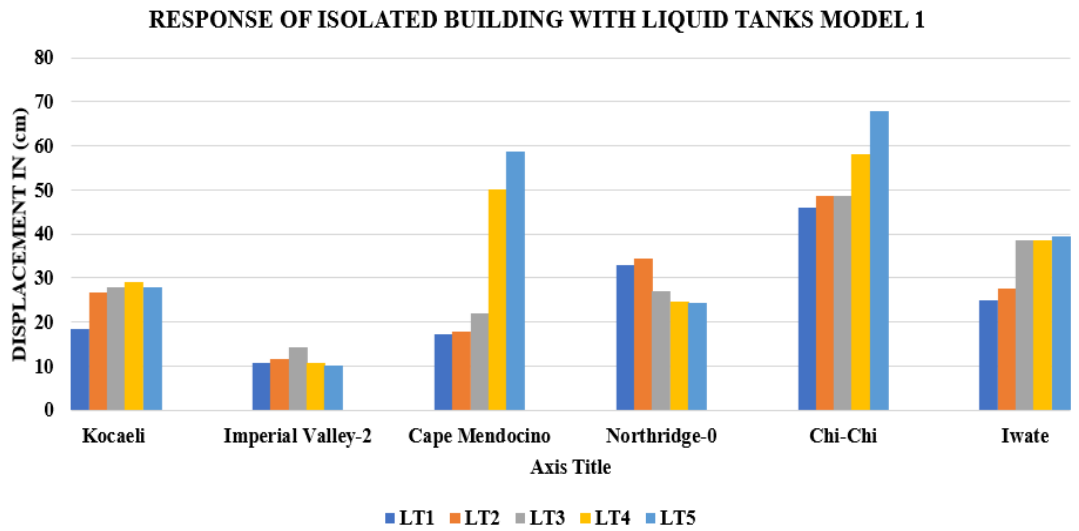


**Figure 5.2** Response of Isolated Building with Liquid Tanks Model 1

#### 5.1.4 Story Drift

Relative story drift in the isolated building is minimized as the super-structure of the isolated buildings almost behave as rigid blocks, and the total displacement is concentrated on the isolators. The story drift is observed to decrease further with the installation of liquid tanks as the liquid tank's sizes and capacity increase. Figure 5.3 represent the five earthquakes that show a reduction of about 57%, 39%, 77%, 62%, and 43% for the Kocaeli, Imperial Vally-02, Northridge, Chi-Chi, and Iwate earthquakes. However, there is a 15% increase for the Cape Mendocino earthquake.

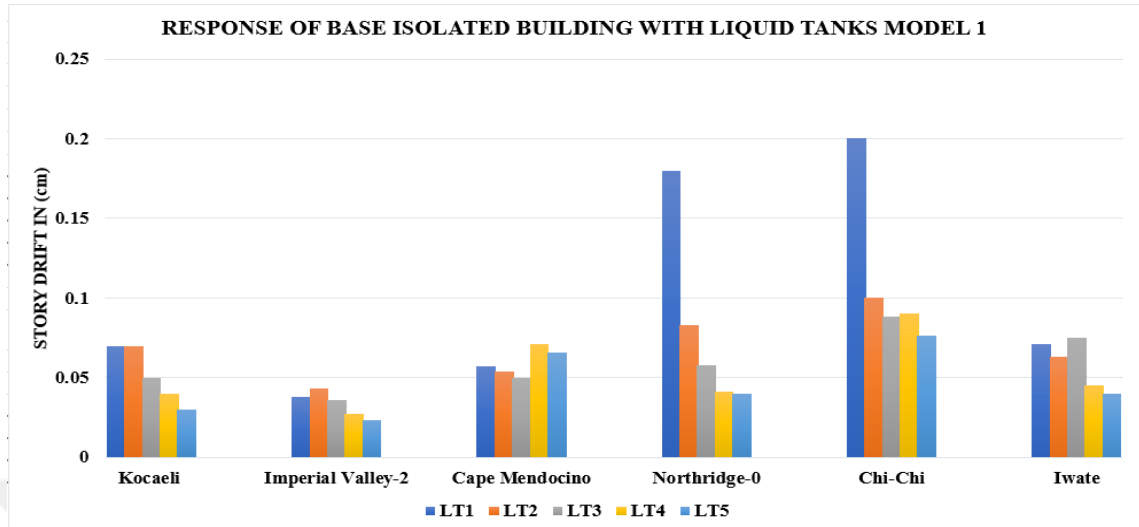


Figure 5.3 Response of Isolated Building with Liquid Tanks Model 1

Table 5.1 Maximum Response Of (LT1 to LT5) for Six Near-Fault Earthquakes

No	Earthquake	RSN	Station Name	Bearing force (kN)	Bearing displacement (cm)	Tank Weight (kN) ( $m_t+m_w$ )	Story drift (cm)	h/L
LT1	Kocaeli Turkey	1165	Izmit.90	120.27	18.43	19.9	0.07	2
LT2				153	26.7	27.5	0.07	3
LT3				158	28	74.6	0.05	2
LT4				164	29	208.4	0.04	4
LT5				162	28	253.1	0.03	5
LT1	Imperial Valley-2	6	El Centro Array #9	88	10.8	19.9	0.038	2
LT2				91	11.5	27.4	0.043	3
LT3				101.42	14.17	74.6	0.036	2
LT4				88.12	10.76	208.4	0.027	4
LT5				85.6	10.2	253.1	0.023	5
LT1	Cape Mendocino	3750	270	114.8	17.3	19.9	0.057	2
LT2				116.39	17.7	27.4	0.054	3
LT3				133.9	22	74.6	0.05	2
LT4				247	50	208.0	0.071	4
LT5				284	58.8	253.1	0.066	5
LT1	Northridge-01	1086	Med,Ff 90	179	33	19.9	0.18	2
LT2				185	34.5	27.4	0.083	3
LT3				154	26.9	74.6	0.058	2
LT4				145	24.7	208	0.041	4
LT5				143.3	24.3	253	0.04	5
LT1	Chi-Chi	1504	Tcu067	232.4	46	19.9	0.2	2
LT2				239	48.7	27.4	0.1	3
LT3				243	48.75	74.6	0.088	2
LT4				281	58	208	0.09	4
LT5				321	67.9	253	0.076	5
LIT1	Iwate	5663	Myg004, EW	147	25	19.9	0.071	2
LT2				157	27.6	27.4	0.063	3
LT3				200	38.5	74.6	0.075	2
LT4				202.7	38.6	208	0.045	4
LT5				205	39.4	253	0.04	5

### 5.1.5 Liquid Tanks Case Two

Case two utilizes of six liquid tanks (LT6, LT7, LT8, LT6R, LT7R, LT8R). In which the first three liquid tanks (LT6, LT7, LT8) are sloshing liquid tanks however the last three liquid tanks (LT6R, LT7R, LT8R) was assumed to have a rigid liquid mass. The size of empty tanks is considered the same for all liquid tanks. Only the height of the water is increased for (LT6 and LT6R) 10 tons (LT7, LT7R) 20 tons and (LT8, LT8R) 30 tons all have exact sizes as (4× 2.5×2.5) m, which is length, width, and height respectively. Table 5.2 shows the structure's response with different LTs model 2 and model 3 under six near-fault ground excitations. The following part will discuss the response of base-isolated buildings in terms of bearing force, bearing displacement, and story drift.

### 5.1.6 Bearing Force

Generally, bearing force of an isolated building increases with increasing the height of the liquid. For large tanks, both sloshing and non-sloshing have a significant bearing response in which the Chi-Chi earthquake indicated a maximum bearing force of (455kN) with LT8, which is a sloshing liquid tank, and (434kN) with LT8R, which is a liquid tank with rigid mass assumption. In contrast, Imperial Valley shows minimum bearing force (81 kN) with LT8 and (85kN) with LT8R.

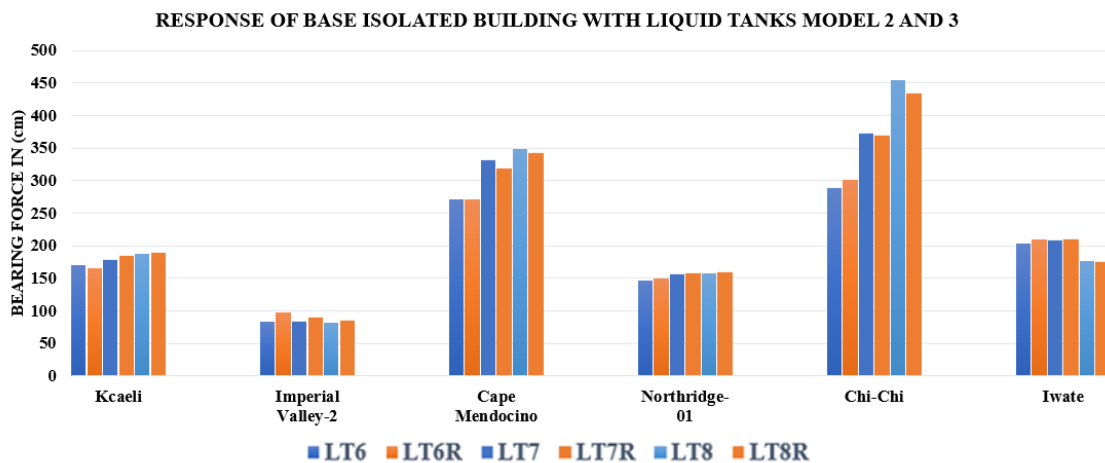


**Figure 5.4** Response of Isolated Building with Liquid Tanks Model 2 And 3

### 5.1.7 Bearing Displacement

It's observed that sloshing liquid tanks have a more bearing displacement response for earthquakes with high PGD. The maximum displacement is observed with LT8 under the Chi-Chi earthquake motion. The minimum displacement was observed with LT8 against Imperial Valley, which is (9cm) as shown in Figure 5.

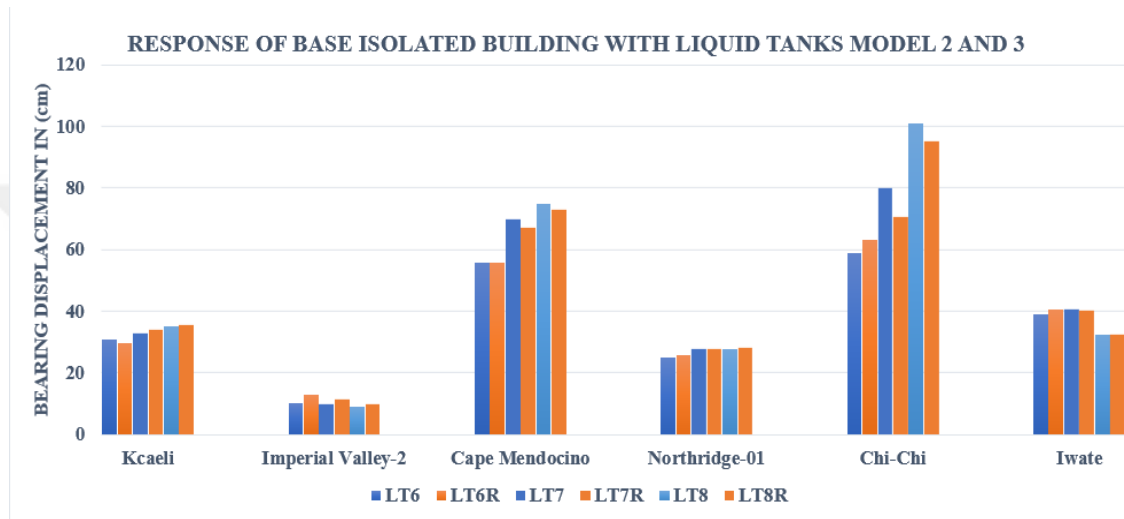


Figure 5.5 Response of Isolated Building with Liquid tanks case two

### 5.1.8 Story Drift

Generally, the isolation system significantly reduces the relative story drift. Similarly, liquid tanks further lessen story drift in such a way that with an increase in the liquid height, the story drift decreases, as shown in figure 5.6.

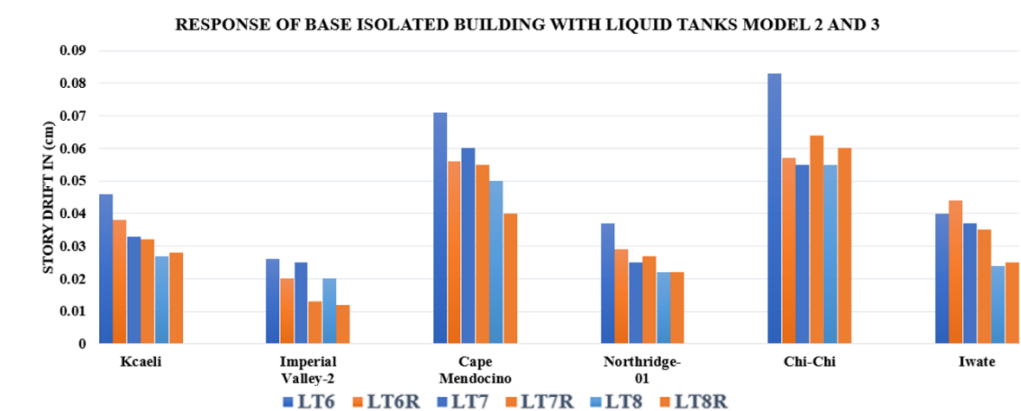
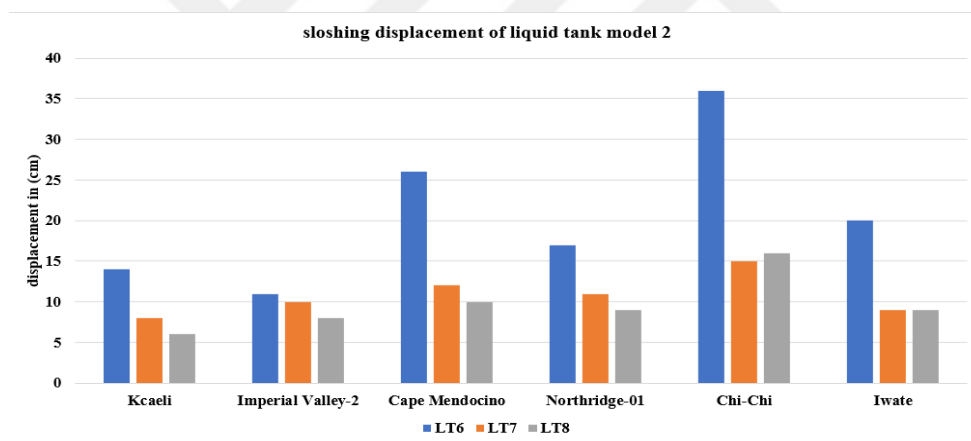


Figure 5.6 Response of Isolated Structure with Liquid tanks case two

### 5.1.9 Sloshing Displacement of Liquid

When a liquid tank is subjected to earthquake excitation, the liquid inside the tank undergoes sloshing motion. The fluid with the tank induces different hydrodynamics pressure on the tank walls. The height of liquid sloshing depends on several factors, such as liquid tank length, liquid depth, and the properties of the earthquake excitation.

In this study, it was observed that the liquid tanks, namely LT6, LT7, and LT8, show a decrease in sloshing liquid Displacement when the liquid height increases in the tanks, as shown in Figure 5.7, where the maximum sloshing height was observed in LT6 under Chi-Chi earthquake excitation. In contrast, the minimum response was observed in LT8 when the structure was subjected to the Kocaeli earthquake.



**Figure 5.7** Response of Isolated Building with Liquid Tanks Model 2

Table 5.2 summarizes maximum response for liquid tanks (LT6, LT7, and LT8)

**Table 5.2** Maximum Response Of (LT6 to LT8) for Six Near-Fault Earthquakes

Liquid Tanks	Earthquake Name	RSN	Station Name	Bearing force (kN)	Bearing disp(cm)	Story drift (cm)	water depth(m)	Sloshing displacement (cm)
LT6				169.6	30.7	0.046	1	14
LT7	Kocaeli turkey	1165	Izmit,90	178	33	0.033	2	8
LT8				187	35	0.027	3	6
LT6				84	10	0.026	1	11
LT7	Imperial valley 2	6	Centro Array #9	83.9	9.74	0.025	2	10
LT8				81	9.13	0.02	3	8
LT6				271	55.6	0.071	1	26
LT7	Cape Mendocino	3750	270	331	70	0.06	2	12
LT8				349	74.7	0.05	3	10
LT6				146.6	25	0.037	1	17
LT7	Northridge-1	1086	Med,Ff 90	156.6	27.6	0.025	2	11
LT8				157.45	27.7	0.022	3	9
LT6				288	59	0.083	1	36
LT7	Chi-Chi	1504	Tcu067, EW	372	80	0.055	2	15
LT8				455	101	0.055	3	16
LT6				204	39	0.04	1	20
LT7	Iwate	5663	Myg004, Ew	209	40.52	0.037	2	9
LT8				176.57	32.44	0.024	3	9

The maximum response of the isolated building for liquid tanks (LT6R, LT7R, and LT8R) presented in Table 5.3.

**Table 5.3** The Response of Isolated Structure with Tanks Model 3

Liquid Tanks	Earthquake name	RSN	Station name	Weight of Water (tons)	Bearing force (kN)	Max Bearing displacement (cm)	Max's Story drift(cm)	Length/depth ratios
LT6R				10	166	29.8	0.038	4
LT7R	Kocaeli Turkey	1165	Izmit,90	20	184	34	0.032	2
LT8R				30	190	35.7	0.028	1.33
LT6R				10	97	13	0.02	4
LT7R	Imperial valley 2	6	Centro Array #9	20	90.4	11.3	0.013	2
LT8R				30	85.7	10	0.012	1.33
LT6R				10	271	55.7	0.056	4
LT7R	Cape Mendocino	3750	270	20	319	67	0.055	1.33
LT8R				30	342	72.9	0.04	
LT6R				10	149.6	25.8	0.029	4
LT7R	Northridge-01	1086	Med, Ff 90	20	157	27.8	0.027	2
LT8R				30	159.8	28.3	0.022	1.33
LT6R				10	301.6	63	0.057	4
LT7R	Chi-Chi	1504	Tcu067, EW	20	369	70.7	0.064	2
LT8R				30	434	95	0.06	1.33
LT6R				10	209	40.4	0.044	4
LT7R	Iwate	5663	Myg004, Ew	20	209.4	40.4	0.035	2
LT8R				30	174.6	32.5	0.025	1.33

## CHAPTER 6

### 6.1 Conclusion

This study investigates the influence of liquid tanks on the seismic response of a base isolated structure. The response history analysis was carried out on a seismically isolated building with various liquid tanks installed on its base level. The isolation system in this study consisted of Lead Rubber Bearing (LRB) isolators. A total of eleven different liquid tanks were used in the analyses. The first case was comprised of five small tanks named (LT1, LT2, LT3, LT4, and LT5) with different aspect ratios. The second case contains six larger tanks titled (LT6, LT7, LT8, LT6R, LT7R, and LT8R) the first three liquid tanks were considered as sloshing liquid tanks however the last three liquid tanks were assumed to have rigid liquid mass the reason behind this assumption is to compare the response of the building using different mechanical analogue of liquid tanks and find out the difference if the sloshing motion of liquid is neglected.

The analysis of the structure subjected to six near-fault ground motions was conducted with MATLAB. Seismic response parameters in this study, included the bearing force, bearing displacement, relative story drift, and sloshing height of the liquid. Finally, a comparative analysis was conducted to determine the critical factors that contribute to the overall response of the structure, and the following significant findings are listed below.

The conclusion was made through the following key findings.

- ❖ Significant changes in bearing displacement and bearing force were observed when the liquid mass was more than 24% of the total mass of the structure.
- ❖ It was observed that the most influential factor which dominates the response of the structure was Peak Ground Displacement (PGD) of earthquake.
- ❖ The response with liquid tanks case two which includes different mechanical analogue (sloshing liquid tanks and tanks with rigid liquid mass assumption) results that it will not make a considerable difference when neglecting sloshing motion of liquid.

- ❖ Inter-story drift of the isolated structure reduces with the increase in the liquid tank's capacity.

## **6.2 Recommendation For Future Studies**

This thesis project mainly investigates the influence of small and large liquid tanks on Lead Rubber Bearing (LRB) isolated buildings in terms of bearing displacement, bearing force, sloshing height of the liquid, and story drift. The experimental validation was not performed in the laboratory on the actual model. This topic is suggested for future research studies.

## REFERENCES

- [1] Winters, C. W., & Constantinou, M. C. (1993). Evaluation of static and response spectrum analysis procedures of SEAOC/UBC for seismic isolated structures. In *Evaluation of static and response spectrum analysis procedures of SEAOC/UBC for seismic isolated structures* (pp. 160-160).
- [2] Özdemir, G. (2010). Response of isolated structures under bi-directional excitations of near-field ground motions.
- [3] Das, A., Maity, D., & Bhattacharyya, S. K. (2022, March). Investigation on the efficiency of deep liquid tanks in controlling dynamic response of high-rise buildings: A computational framework. In *Structures* (Vol. 37, pp. 1129-1141). Elsevier.
- [4] Novo, T., Varum, H., Teixeira-Dias, F., Rodrigues, H., Silva, M. F., Costa, A. C., & Guerreiro, L. (2014). Tuned liquid dampers simulation for earthquake response control of buildings. *Bulletin of earthquake engineering*, 12(2), 1007-1024.
- [5] Furtmüller, T., Di Matteo, A., Adam, C., & Pirrotta, A. (2019). Base-isolated structure equipped with tuned liquid column damper: An experimental study. *Mechanical Systems and Signal Processing*, 116, 816-831..
- [6] Chang, Y., Noormohamed, A., & Mercan, O. (2018). Analytical and experimental investigations of modified tuned liquid dampers (MTLDs). *Journal of Sound and Vibration*, 428, 179-194.
- [7] Ashasi-Sorkhabi, A., Malekghasemi, H., Ghaemmaghani, A., & Mercan, O. (2017). Experimental investigations of tuned liquid damper-structure interactions in resonance considering multiple parameters. *Journal of Sound and Vibration*, 388, 141-153.
- [8] Ruiz, R. O., Lopez-Garcia, D., & Taflanidis, A. A. (2016). Modeling and experimental validation of a new type of tuned liquid damper. *Acta Mechanica*, 227(11), 3275-3294.
- [9] Pabarja, A., Vafaei, M., Alih, S. C., Yatim, M. Y. M., & Osman, S. A. (2019). Experimental study on the efficiency of tuned liquid dampers for vibration mitigation of a vertically irregular structure. *Mechanical Systems and Signal Processing*, 114, 84-105.
- [10] Zhang, Z. (2020). Numerical and experimental investigations of the sloshing modal properties of sloped-bottom tuned liquid dampers for structural vibration control. *Engineering Structures*, 204, 110042.
- [11] Pandey, D. K., Sharma, M. K., & Mishra, S. K. (2019). A compliant tuned liquid damper for controlling seismic vibration of short period structures. *Mechanical Systems and Signal Processing*, 132, 405-428.
- [12] Fei, Z., Jinting, W., Feng, J., & Liqiao, L. (2019). Control performance comparison between tuned liquid damper and tuned liquid column damper using real-time hybrid simulation. *Earthquake Engineering and Engineering Vibration*, 18(3), 695-701.
- [13] Shin, J. H., Kwak, M. K., Kim, S. M., & Baek, K. H. (2020). Vibration control of multi-story building structure by hybrid control using tuned liquid damper and active mass damper. *Journal of Mechanical Science and Technology*, 34(12), 5005-5015. Figure 1. 1.

- [14] McNamara, K. P., Love, J. S., & Tait, M. J. (2022). Numerical investigation of the response of structures equipped with a limited freeboard tuned liquid damper. *Journal of Fluids and Structures*, 108, 103426.
- [15] Bhattacharjee, E., Halder, L., & Sharma, R. P. (2013). An experimental study on tuned liquid damper for mitigation of structural response. *International Journal of Advanced Structural Engineering*, 5(1), 1-8.
- [16] Tang, Z., Dong, Y., Liu, H., & Li, Z. (2022). Frequency domain analysis method of tuned liquid damper controlled multi-degree of freedoms system subject to earthquake excitation. *Journal of Building Engineering*, 48, 103910.
- [17] Naeim, F., & Kelly, J. M. (1999). *Design of seismic isolated structures: from theory to practice*. John Wiley & Sons.
- [18] Robinson, W. H. (2000). Seismic isolation of civil buildings in New Zealand. *Progress in Structural Engineering and Materials*, 2(3), 328-334.
- [19] Constantinou, M. C., Whittaker, A. S., Kalpakidis, Y., Fenz, D. M., & Warn, G. P. (2007). Performance of seismic isolation hardware under service and seismic loading. *Technical Rep. No. MCEER-07, 12*.
- [20] Symans, M. (2005). Instructional Material Complementing FEMA 451, Design Examples. *Rensselaer Polytechnic Institute*.
- [21] Nguyen, V. T., Vu, N. Q., & Nguyen, X. D. (2020, December). Application of seismic isolation for multi-story buildings in moderate seismicity areas like Vietnam. In *Journal of Physics: Conference Series* (Vol. 1706, No. 1, p. 012119). IOP Publishing.
- [22] Konstantinidis, D., & Nikfar, F. (2015). Seismic response of sliding equipment and contents in base-isolated buildings subjected to broadband ground motions. *Earthquake Engineering & Structural Dynamics*, 44(6), 865-887.
- [23] Kanbir, Z., Özdemir, G., & Alhan, C. (2018). Modeling of Lead Rubber Bearings via 3D-BASIS, SAP2000, and OpenSees Considering Lead Core Heating Modeling Capabilities. *International Journal of Structural and Civil Engineering Research*, 7(4), 294-301.
- [24] Yao, X., Meng, L., Chu, P., & Yao, L. (2021). Modeling research and test verification of the seismic response of a multistage series liquid tank. *Shock and Vibration*, 2021.
- [25] Hadj-Djelloul, N., Djermane, M., Sharari, N., & Merabti, S. (2020). Dynamic Behavior of Elevated Water Tanks under Seismic Excitation. *Journal of Engineering and Applied Sciences Technology. SRC/JEAST-114*, 3.
- [26] Maity, D., Satya Narayana, T., & Saha, U. K. (2009). Dynamic response of liquid storage elastic tanks with baffle. *J Struct Eng*, 36(3), 172-181.
- [27] Housner, G. W. (1963). The dynamic behavior of water tanks. *Bulletin of the seismological society of America*, 53(2), 381-387.
- [28] Malhotra, P. K., Nimse, P., & Meekins, M. (2014). Seismic sloshing in a horizontal liquid storage tank. *Structural Engineering International*, 24(4), 466-473.
- [29] Jain, S. K., & Jaiswal, O. R. (2007). IITK-GSDMA guidelines for seismic design of liquid storage tanks. *National Information Centre of Earthquake Engineering, Kanpur*.

- [30] (American Society of Civil Engineers. (2017, June). Minimum design loads and associated criteria for buildings and other structures. American Society of Civil Engineers.
- [31] [peer.berkeley.edu/ngawest2](http://peer.berkeley.edu/ngawest2)
- [32] Isik, E. (2016). Consistency of the rapid assessment method for reinforced concrete buildings. *Earthquakes and Structures*, 11(5), 873-885.
- [33] IITK, I. (2005). GSDMA Guidelines for Seismic Design of Liquid Storage Tanks—Provisions with Commentary and Explanatory Examples. *Indian Institute of Technology Kanpur, Kanpur, India*.
- [34] Soyluk, A., & Harmankaya, Z. Y. (2012). The history of development in Turkish seismic design codes. *International Journal of Civil & Environmental Engineering*, 12(1), 25-29.
- [35] Verma, A., Gupta, A.K., & Nath, P.B. (2017). Base Isolation System: A Review.
- [36] Mostaghel, N., & Tanbakuchi, J. (1983). Response of sliding structures to earthquake support motion. *Earthquake engineering & structural dynamics*, 11(6), 729-748.
- [37] Girish, M., & Pranesh, M. (2013, February). Sliding isolation systems: state-of-the-art review. In *Second International Conference on Emerging Trends in Engineering (SICETE)* (pp. 30-35).
- [38] Kelly, J. M. (1997). Seismic isolation for earthquake-resistant design. In *Earthquake-Resistant Design with Rubber* (pp. 1-18). Springer, London.
- [39] Zayas, V. A., Low, S. S., & Mahin, S. A. (1990). A simple pendulum technique for achieving seismic isolation. *Earthquake spectra*, 6(2), 317-333.
- [40] Veletsos, A. S. (1974, June). Seismic effects in flexible liquid storage tanks. In *Proceedings of the 5th world conference on earthquake engineering* (Vol. 1, pp. 630-639). McLean, VA, USA: Bulletin of the Seismological Society of America.
- [41] Kalpakidis, I. V. (2008). *Effects of heating and load history on the behavior of lead-rubber bearings*. State University of New York at Buffalo.
- [42] Kotrasová, K., & Kormaníková, E. (2017). Liquid Storage Cylindrical Tank-Earthquake Analysis. In *MATEC Web of Conferences* (Vol. 125, p. 04009). EDP Sciences.
- [43] Newmark, N. M. (1974). *Fundamentals of earthquake engineering*. *Printice Hall*.

## APPENDIX

In the last section of this thesis, the complete response history for various aspects of the analysis is provided, including bearing force, bearing Displacement, story drift, and the Displacement of convective mass of water for the whole period of the excitation up to 70 seconds for all six sets of near-fault earthquakes.

### Case One

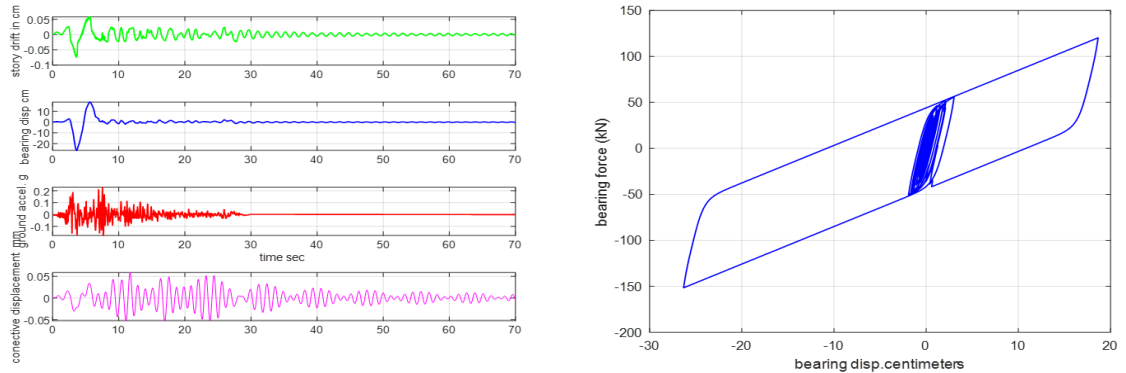


**Figure I** The Response of Structure with LT1 Under Kocaeli Izmit,90,

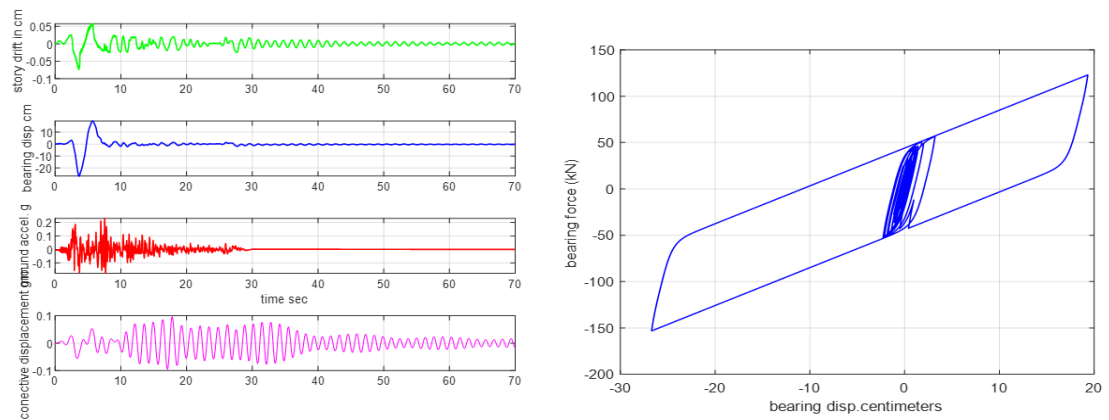


**Figure II** The Response of Structure with LT2 Under Kocaeli, Izmit,90

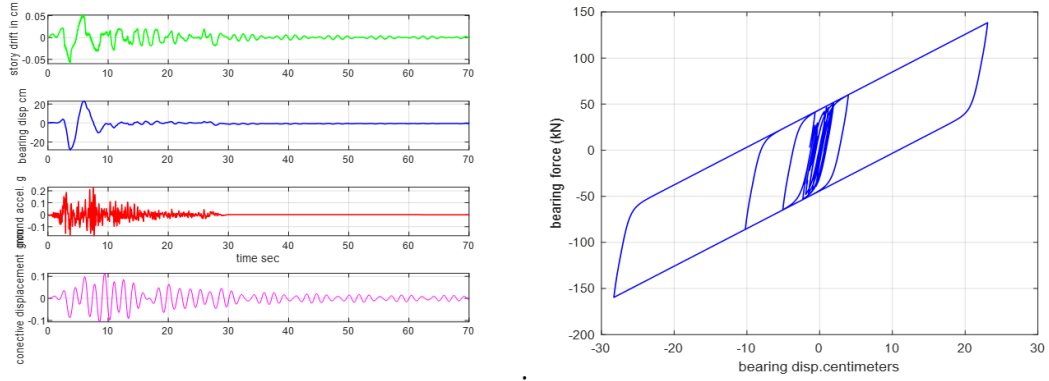


**Figure III** The Response of Structure with LT3 Under Kocaeli, Izmit,90

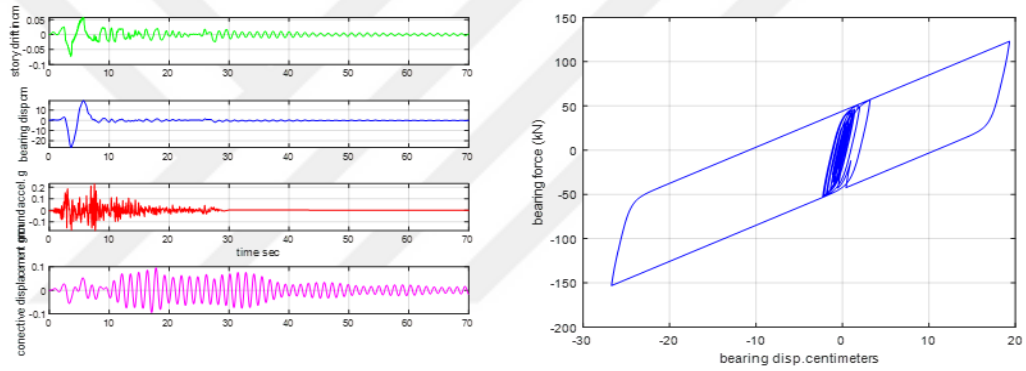


**Figure IV** The Response of Structure with LT4 Under Kocaeli, Izmit,90

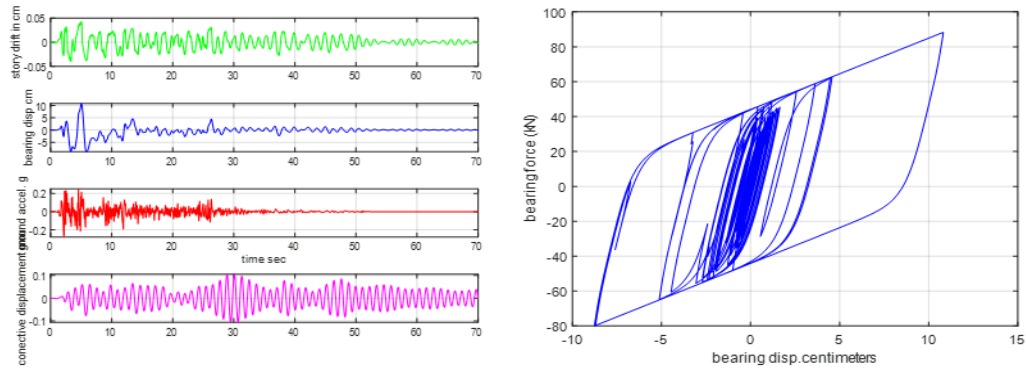


**Figure V** The Response of Structure with LT1 Under El Centro Array #9, 180

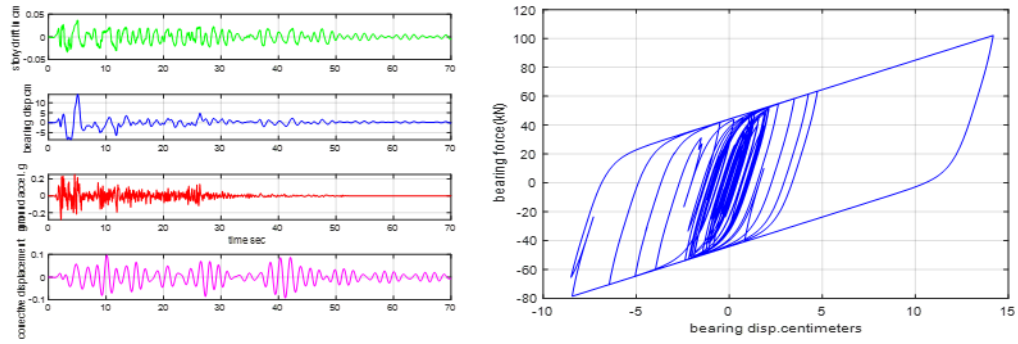


**Figure VI** The Response of Structure with LT2 Under El Centro Array #9, 180

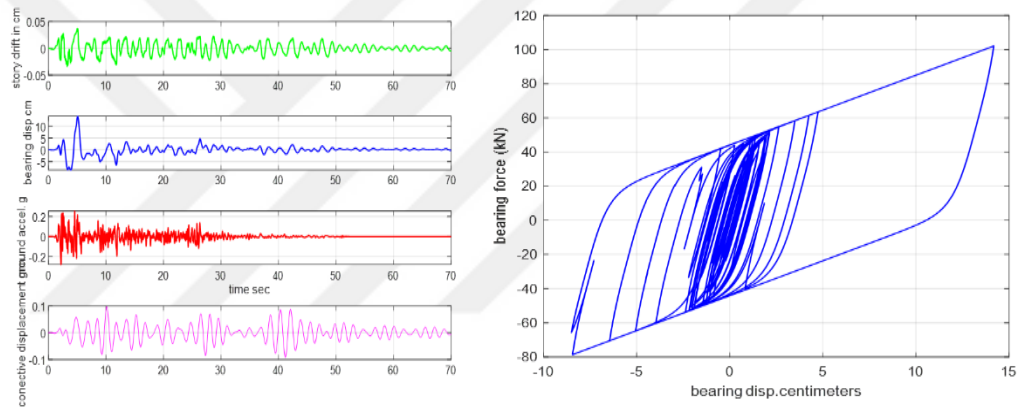


**Figure VII** The Response of Structure with LT3 Under El Centro Array #9, 180

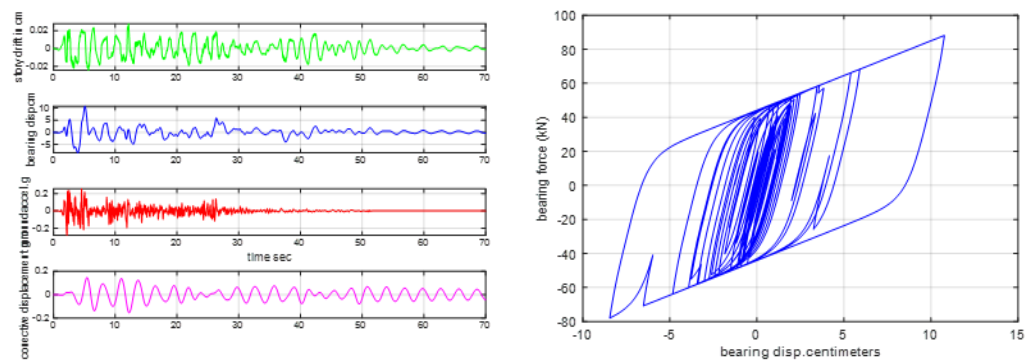


**Figure VIII** The Response of Structure with LT4 Under El Centro Array #9, 180

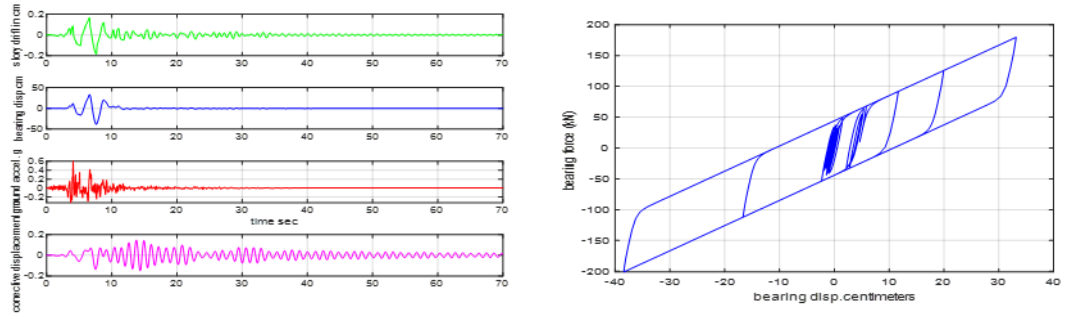


**Figure IX** Response of The Structure for LT1 Under Northridge-01Ff, 90

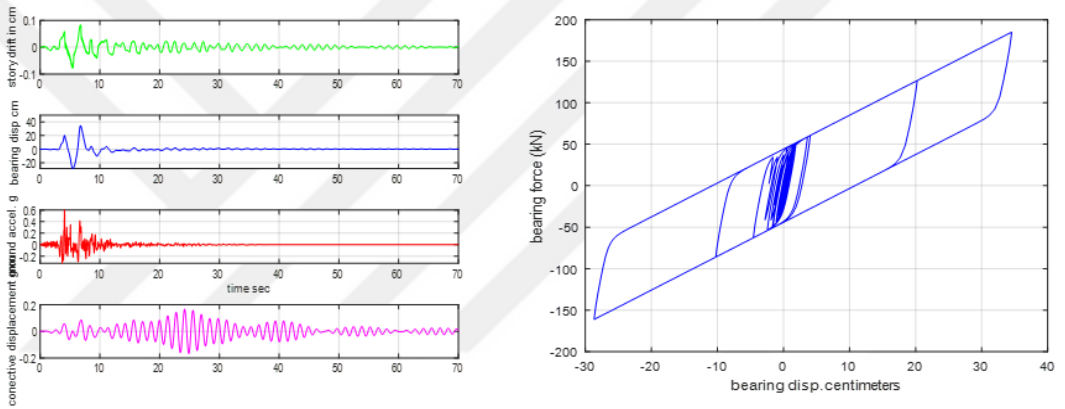


**Figure X** Response of Structure for LT2 Under Northridge-01 Ff, 90

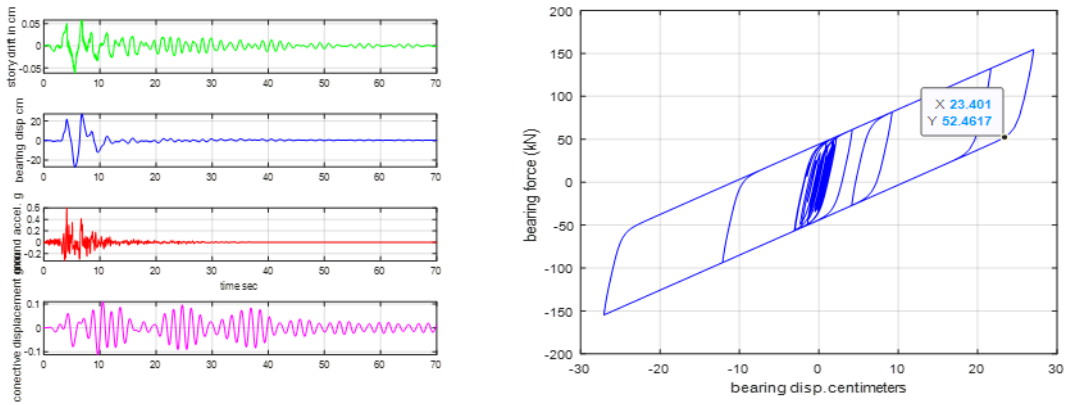


**Figure XI** Response of Structure for LT3 Under Northridge-01 Ff, 90

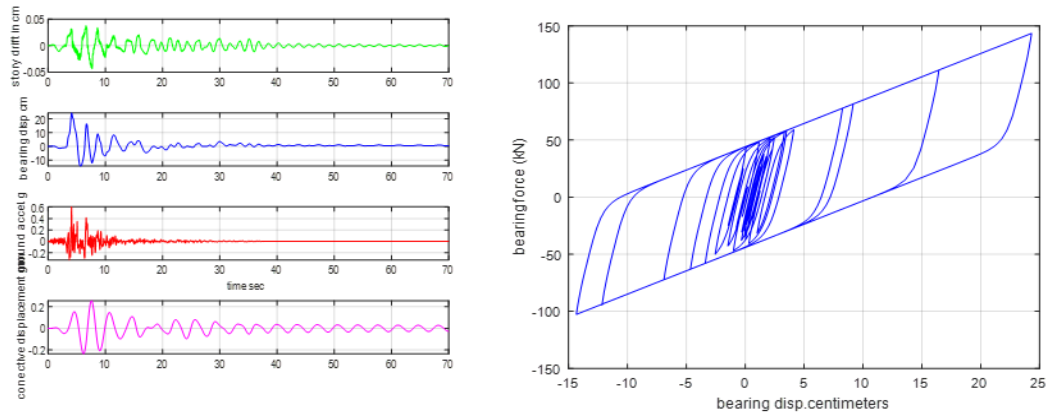


**Figure XII** Response of The Structure for LT4 Under Northridge-01 Ff, 90

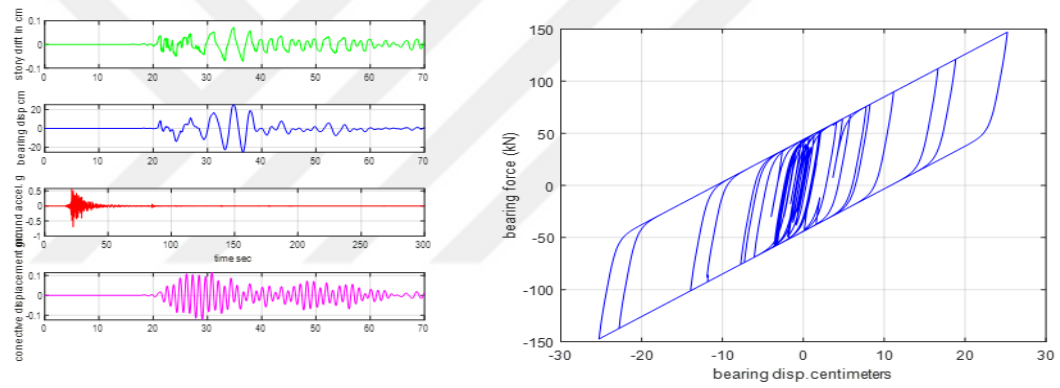


**Figure XIII** The Response of Structure with LT1 under Iwate Myg004, Ew

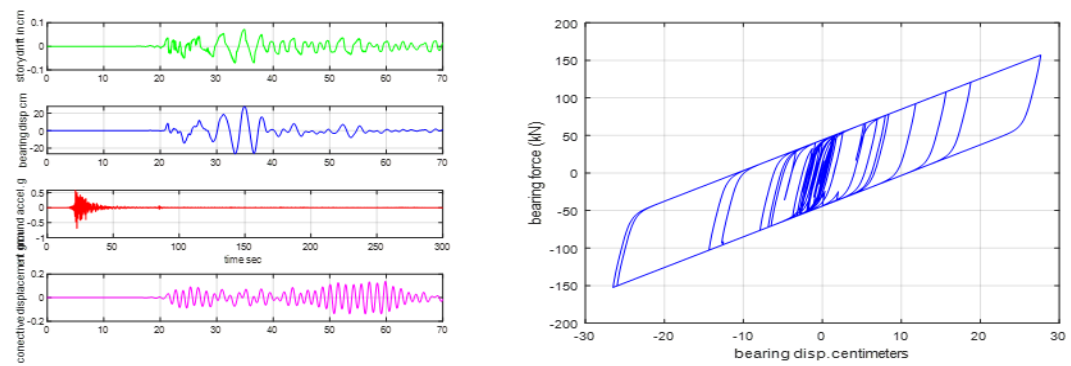


**Figure XIV** The Response of Structure with LT2 under Iwate, Myg004, Ew

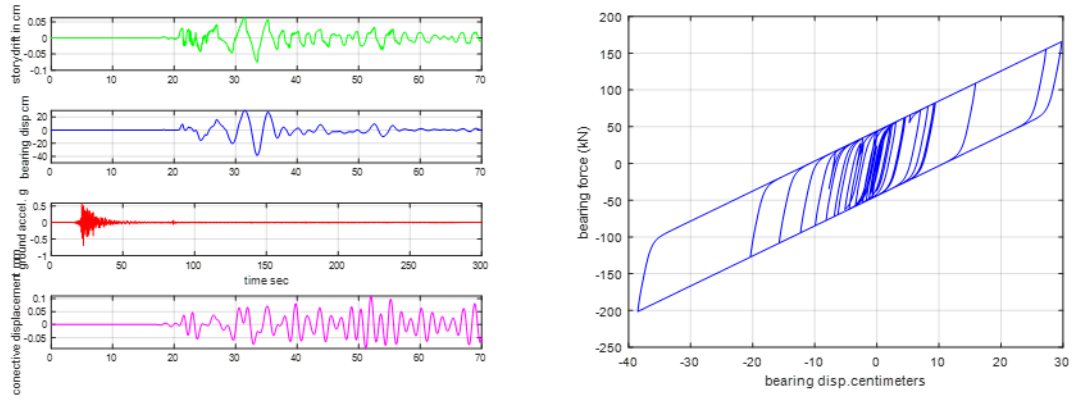


**Figure XV** The Response of Structure with LT3 under Iwate, Myg004, Ew

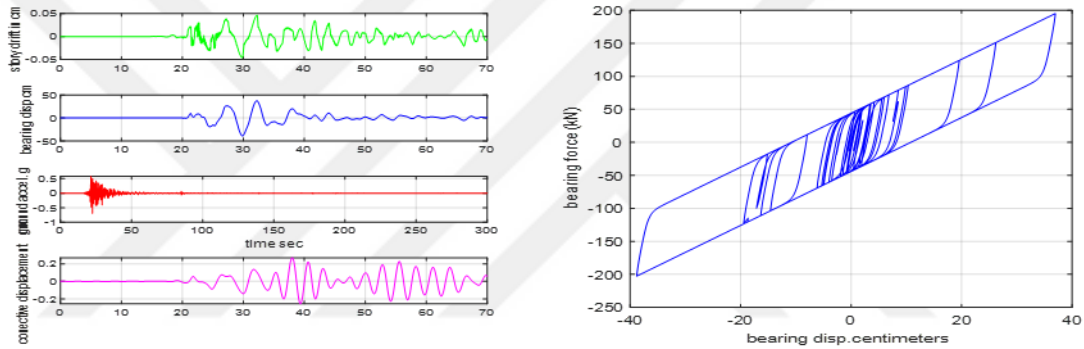


**Figure XVI** The Response of Structure with LT4 under Iwate, Myg004, Ew

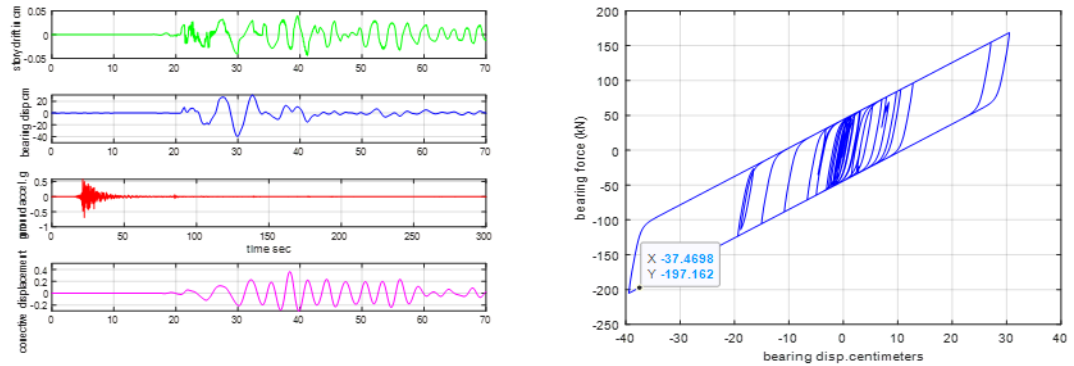


**Figure XVII** The Response of Structure with LT5 under Iwate, Myg004, Ew

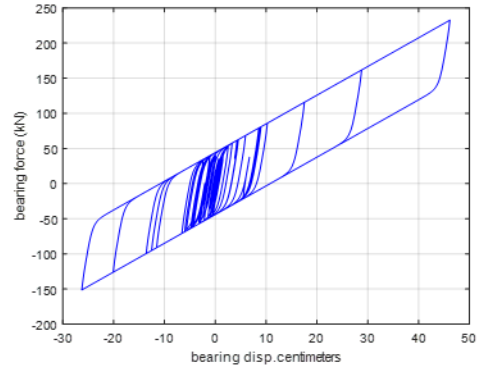
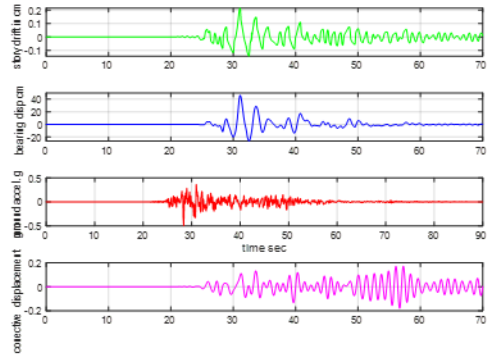


**Figure XVIII** The Response of Structure with LT1 To Chi-Chi Tcu067, E

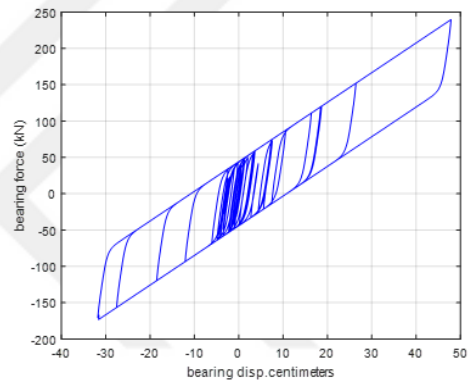
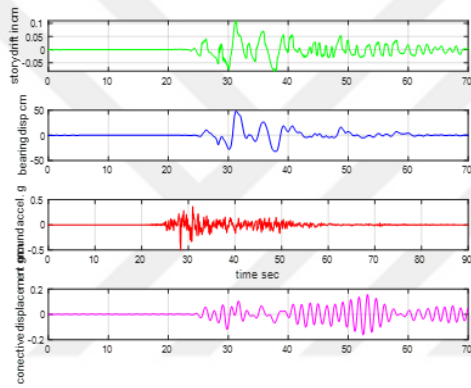


**Figure XIX** The Response of Structure with LT2 To Chi-Chi Tcu067, E

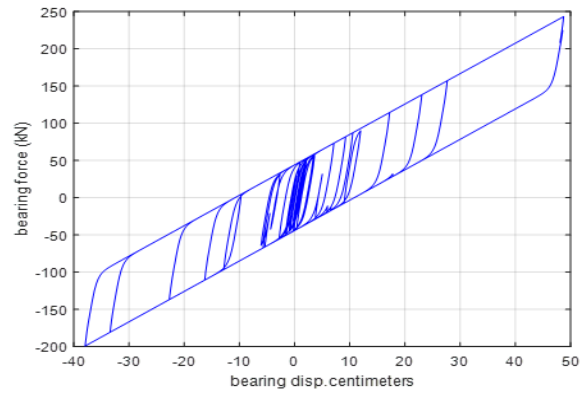
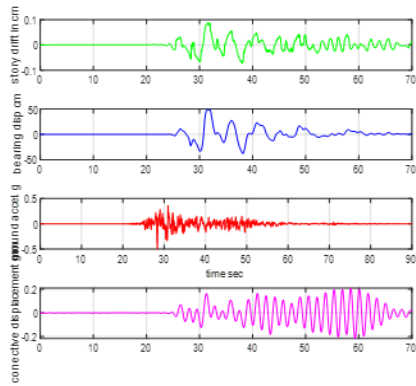


**Figure XX** The Response of Structure with LT3 To Chi-Chi Tcu067, E

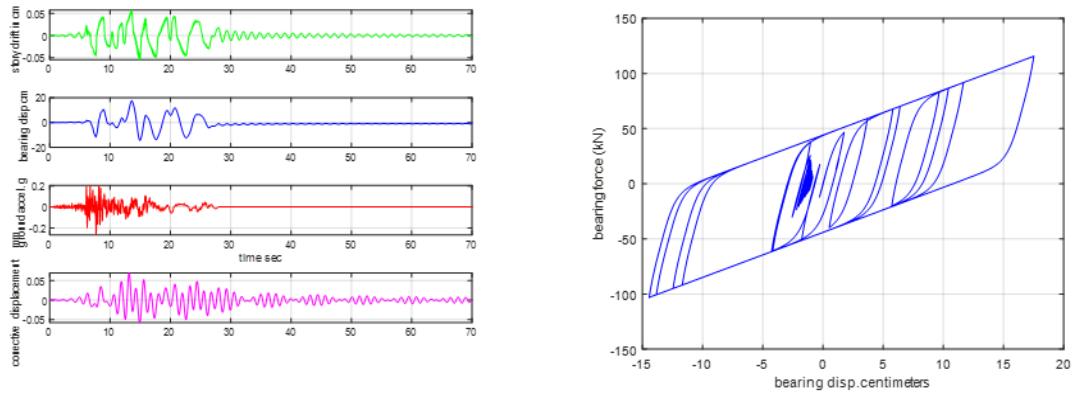


**Figure XXI** The Response of Structure with LT1 To Cape Mendocino,270

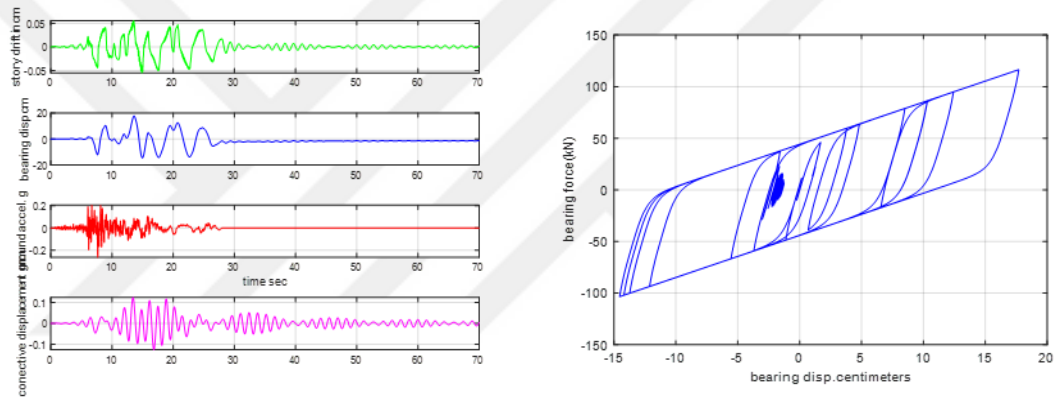


**Figure XXII** The Response of Structure with LT2 To Cape Mendocino,270

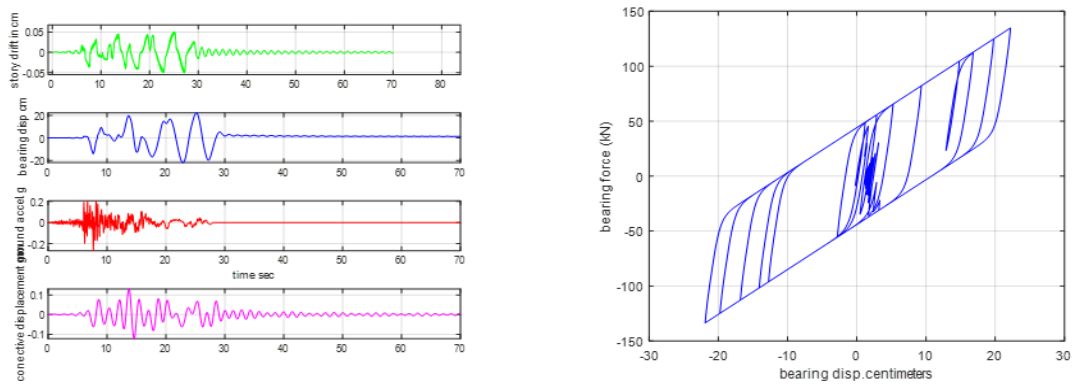


**Figure XXIII** The Response of Structure with LT3 To Cape Mendocino,270

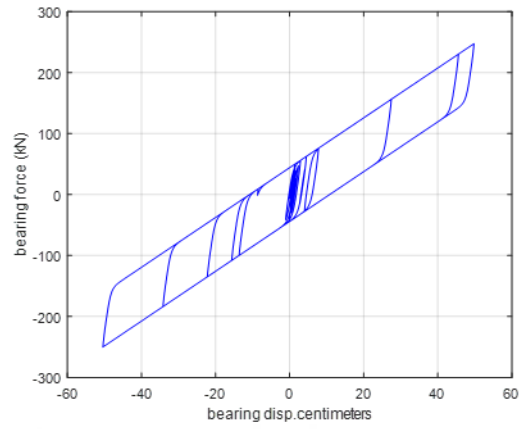
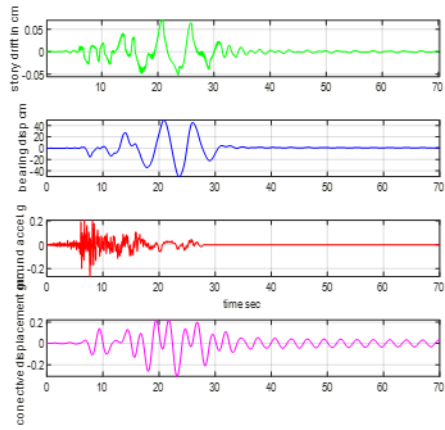


**Figure XXIV** The Response of Structure with LT4 To Cape Mendocino,270

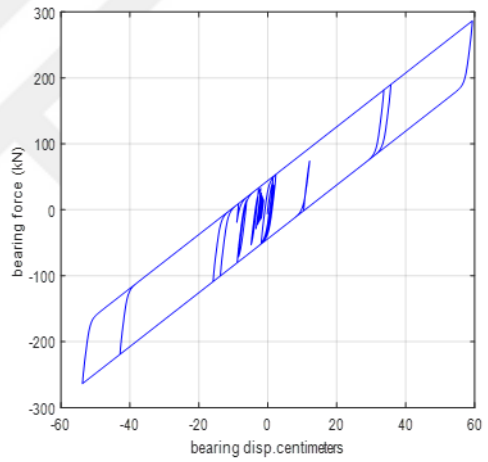
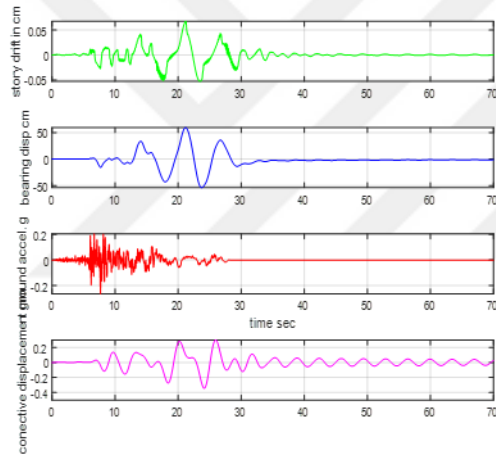


**Figure XXV** The Response of Structure with LT4 To Cape Mendocino,270

## Case Tow

Response of the isolated structure, when large tanks were used following graph, describes the response of the isolated base structure with Liquid Storage tanks named (LT6, LT7, LT8) under six near-fault earthquakes.

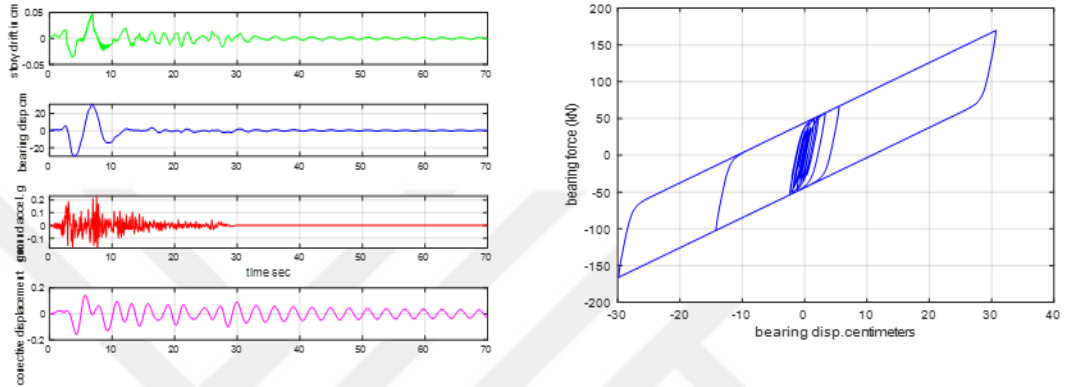


**Figure XXVI** The Response of Structure with LT6 Under Kocaeli Izmit,90

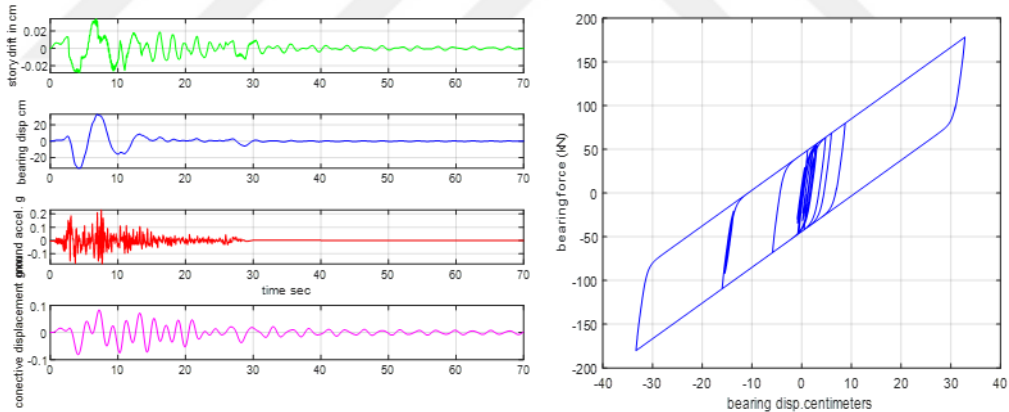


**Figure XXVII** The Response of Structure with LT7 Under Kocaeli Izmit,90

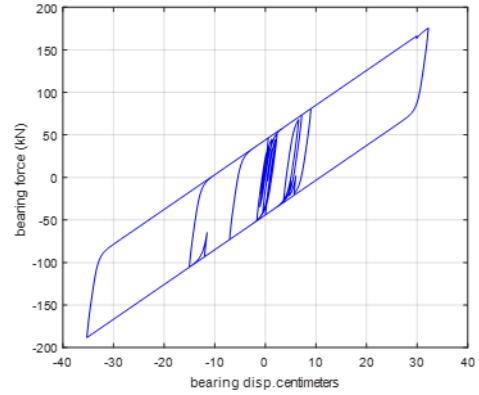
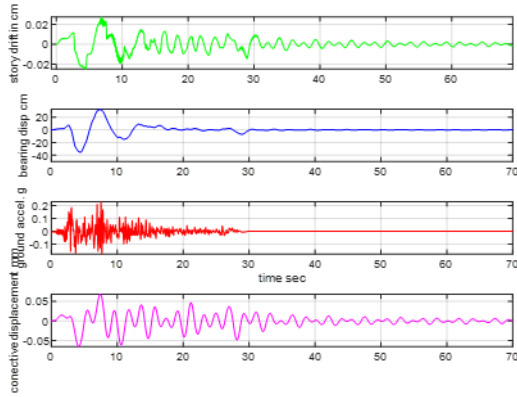


**Figure XXVIII** The Response of Structure with LT8 Under Kocaeli Izmit,90

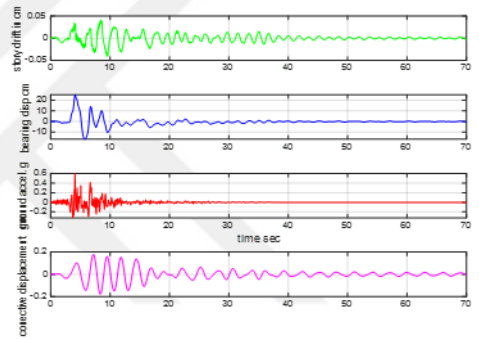
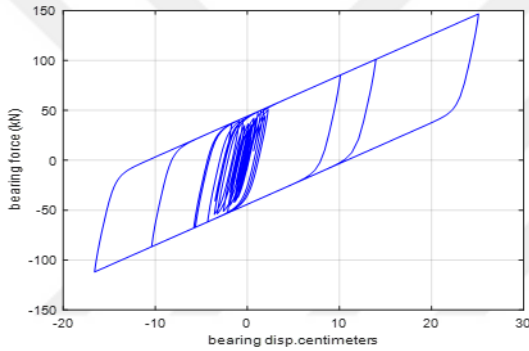


**Figure XXIX** The Structural Response with LT6 Under Northridge-01 Ff, 90

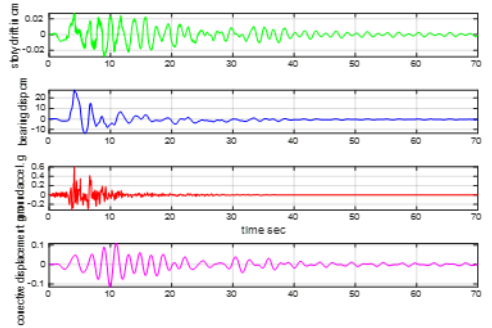
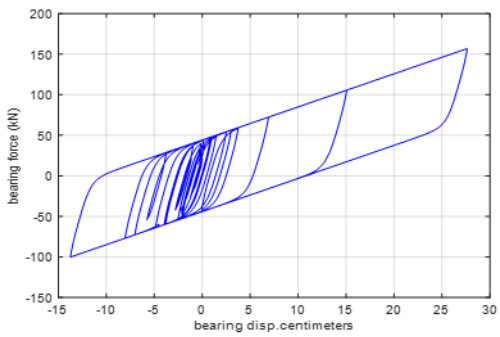


**Figure XXX** The Structural Response with LT7 Under Northridge-01 Ff, 90

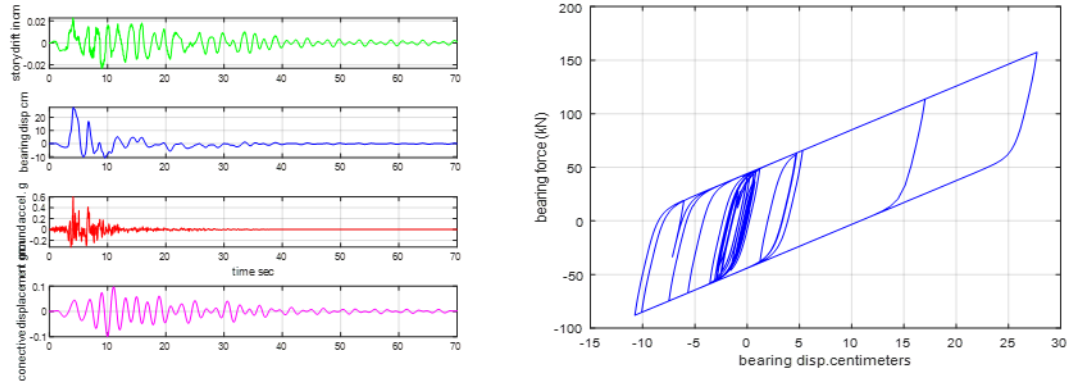


**Figure XXXI** The Structural Response with LT8 Under Northridge-01 Ff, 90

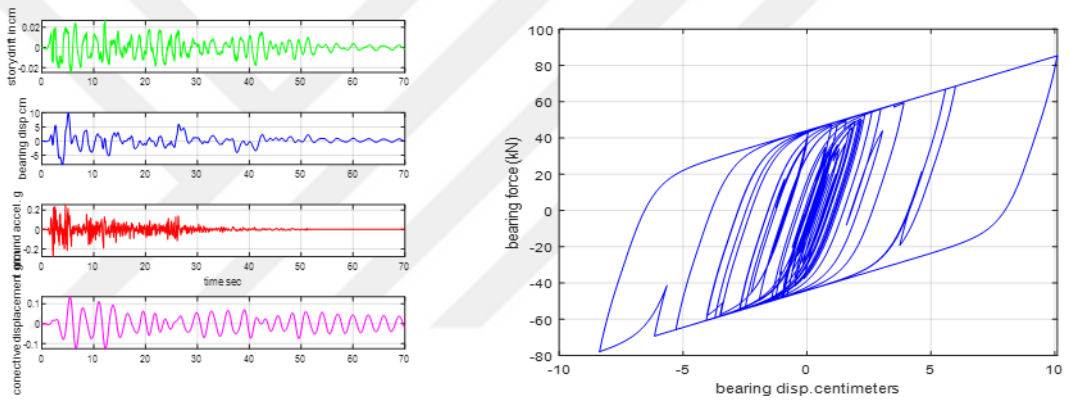


**Figure XXXII** Response of Structure with (LT6) Under El Centro Array #9, 180

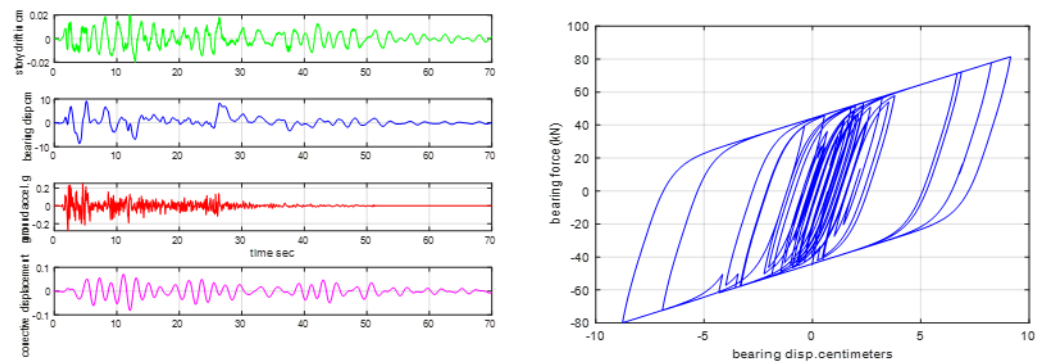


**Figure XXXIII** Response of Structure with (LT7) Under El Centro Array #9, 180

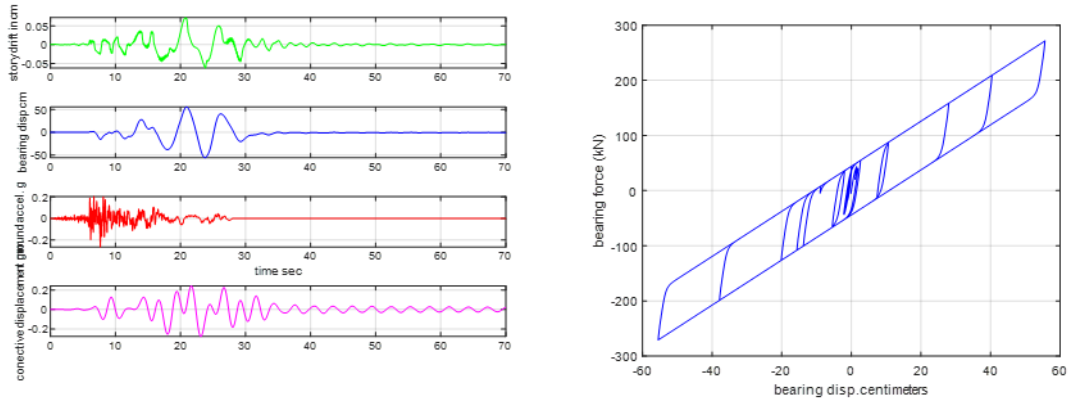


**Figure XXXIV** The Response of Structure With (LT6) to Cape Mendocino, 270

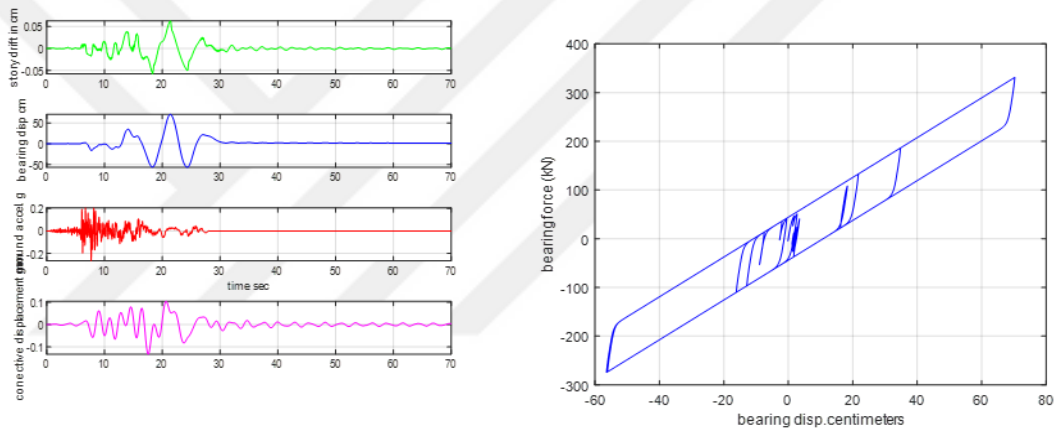


**Figure XXXV** The Response of Structure with LT7 to Cape Mendocino, 270

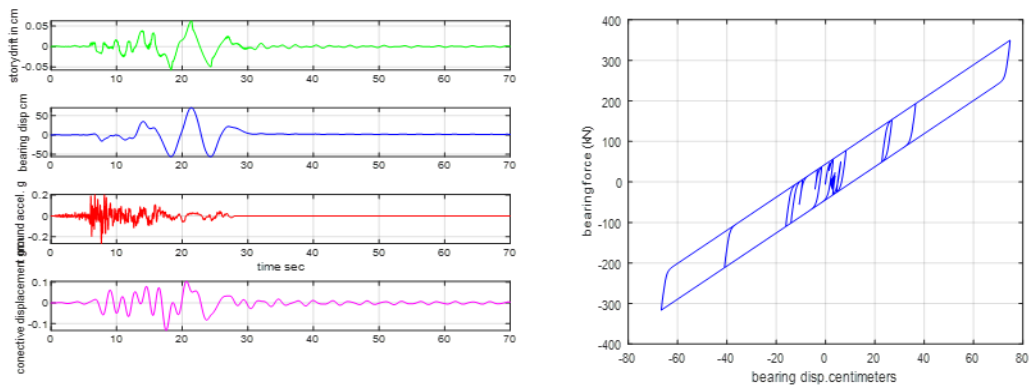


**Figure XXXVI** The Response of Structure with LT7 to Cape Mendocino, 270

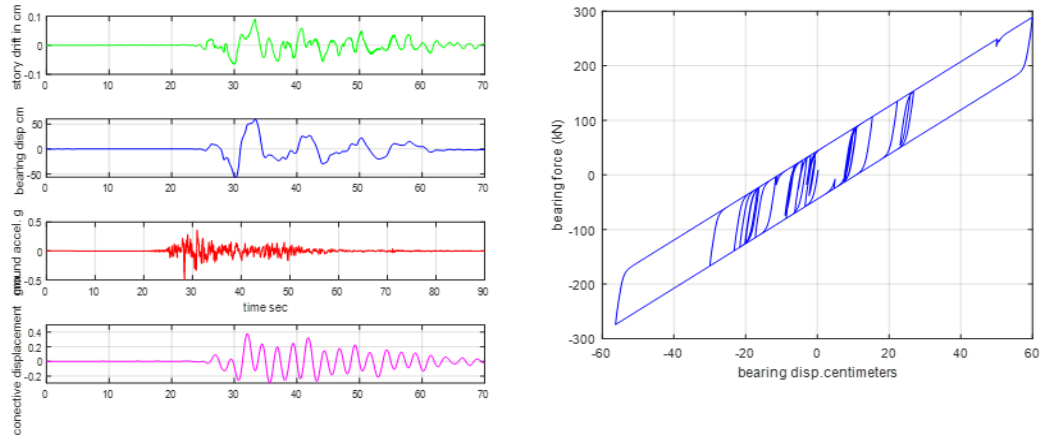


**Figure XXXVII** The Response of Structure with LT6 to the Chi-Chi Tcu067, E

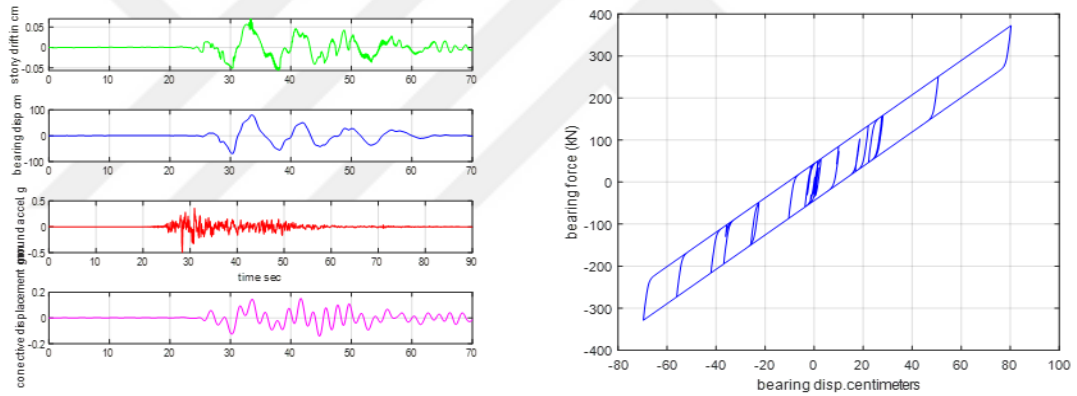


**Figure XXXVIII** The Response of Structure with LT7 to the Chi-Chi Tcu067, E

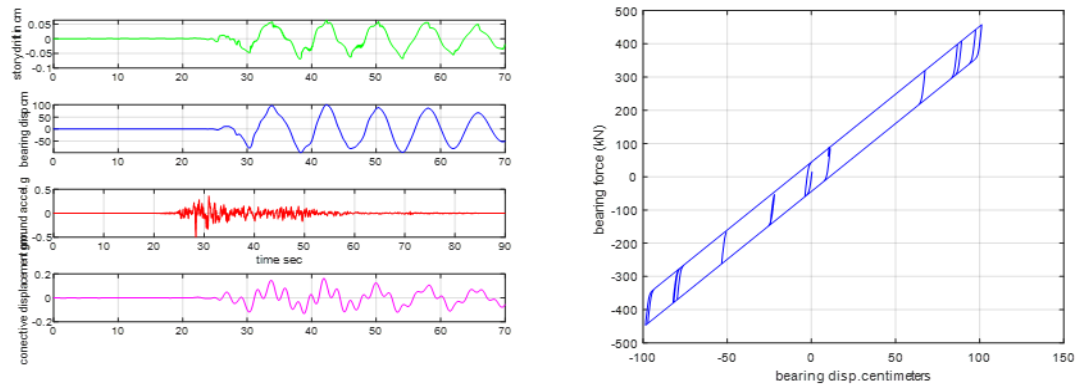


**Figure XXXIX** The Response of Structure with LT8 to the Chi-Chi Tcu067, E

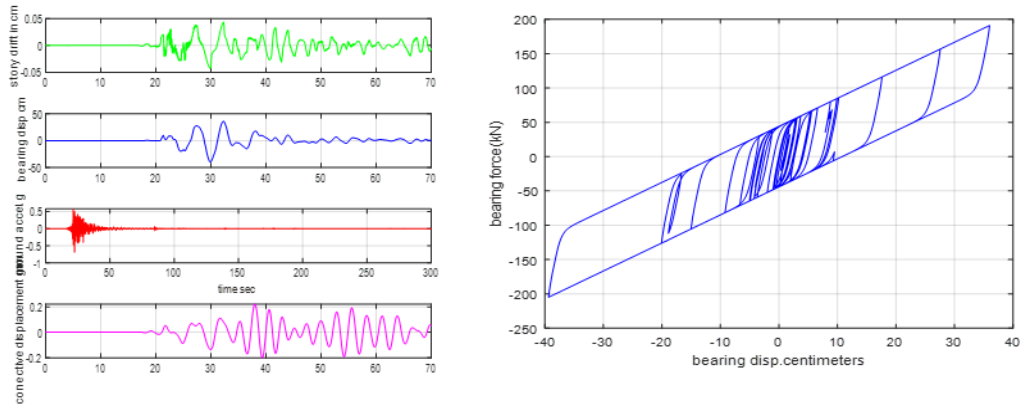


**Figure XL** The Response of Structure with LT6 to Iwate, Myg004, Ew

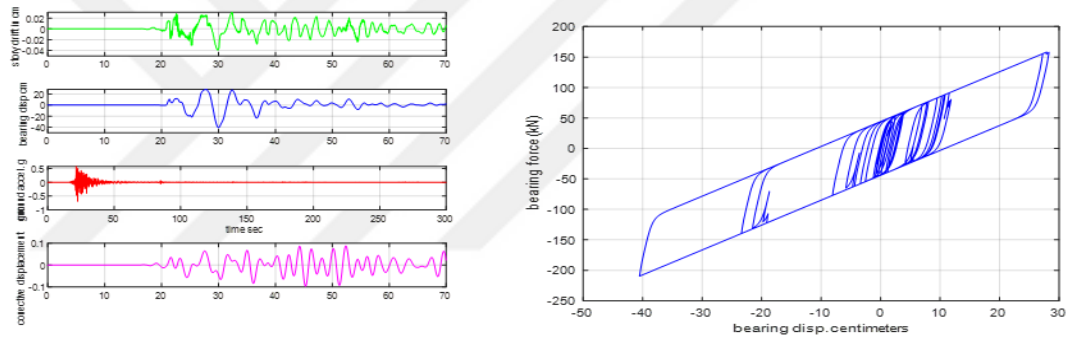


**Figure XLI** The Response of Structure with LT7 to Iwate, Myg004, Ew

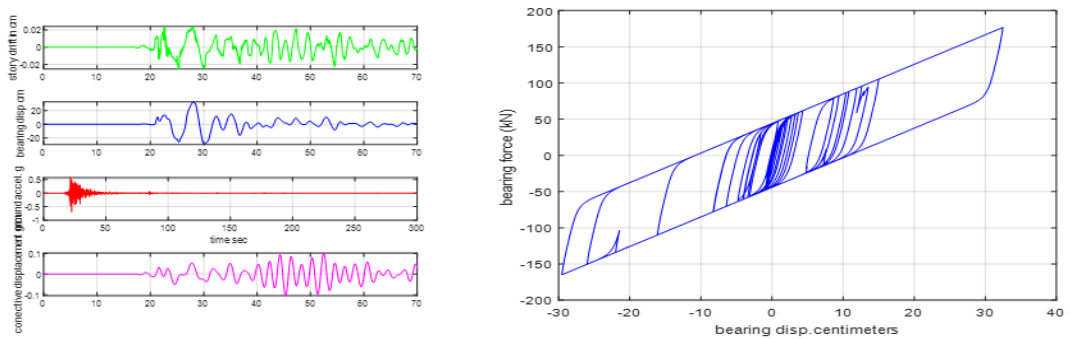


**Figure XLII** The Response of Structure with LT8 to Iwate, Myg004, Ew

### Case Three

Here the structure's response will be shown when Liquid Storage Tanks of the same sizes are used, but it will be assumed to have a non-sloshing motion.

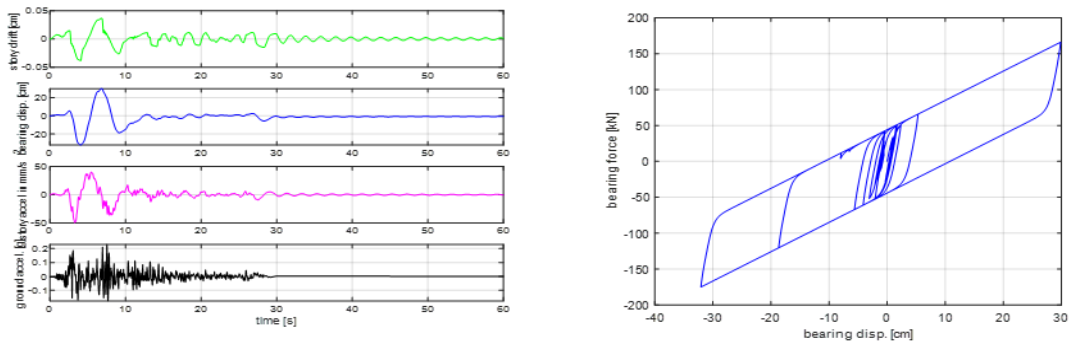


**Figure XLIII** The Response of Structure with LT6R Under Kocaeli Izmit,90

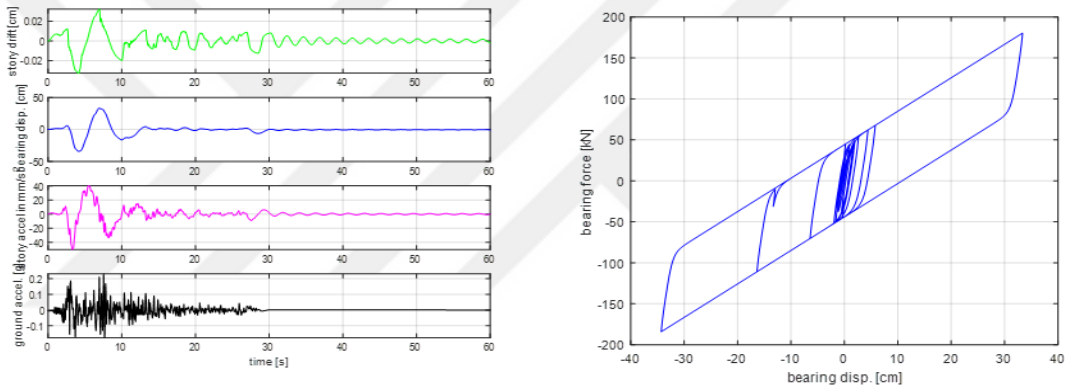


**Figure XLIV** The Response of Structure with LT7R Under Kocaeli Izmit,90

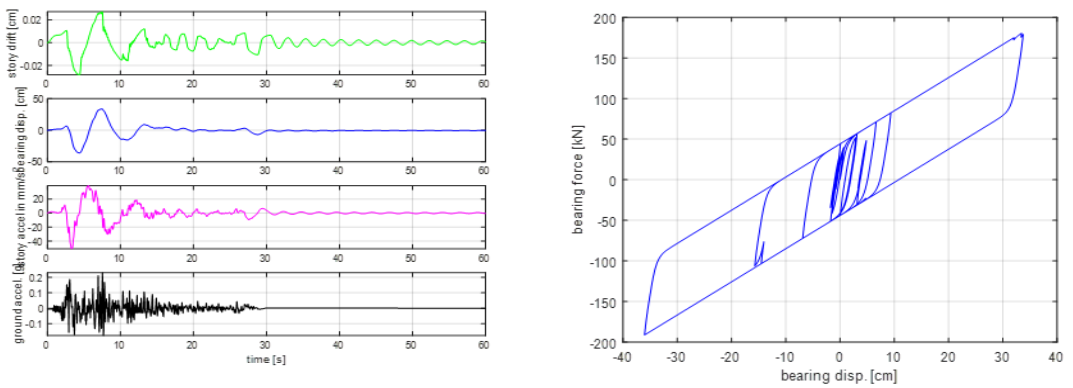


**Figure XLV** The Response of Structure with LT8R Under Kocaeli Izmit,90

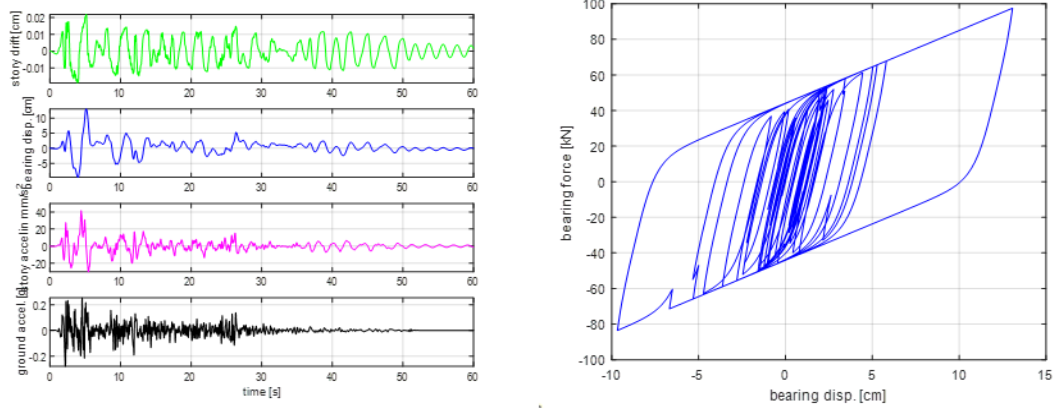


**Figure XLVI** Response of Structure with LT6R Under El Centro Array #9, 180

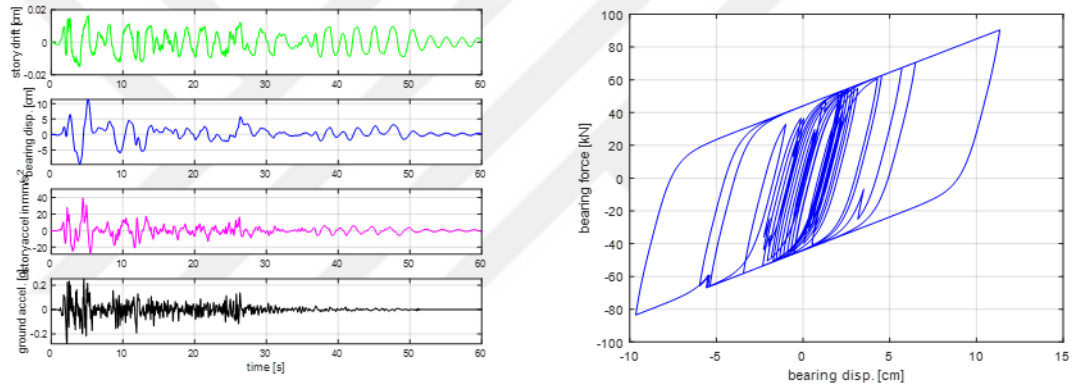


**Figure XLVII** Response of Structure with LT7R Under El Centro Array #9, 180

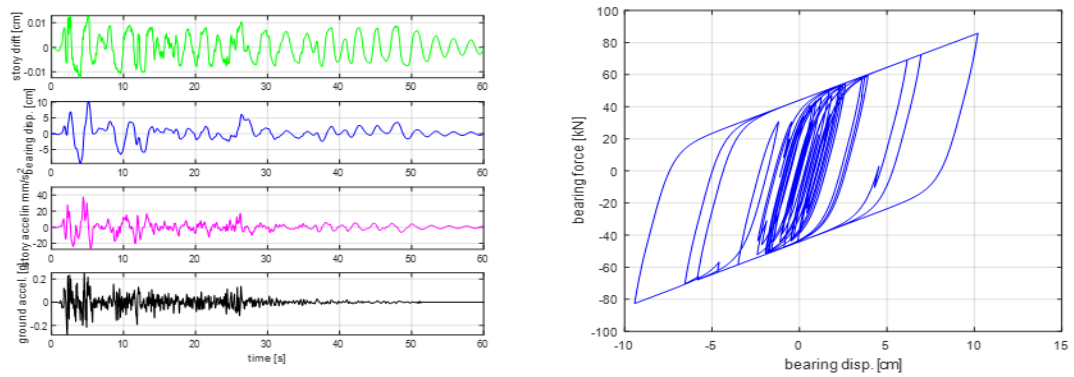


**Figure XLVIII** Response of Structure with LT8R Under El Centro Array #9, 180

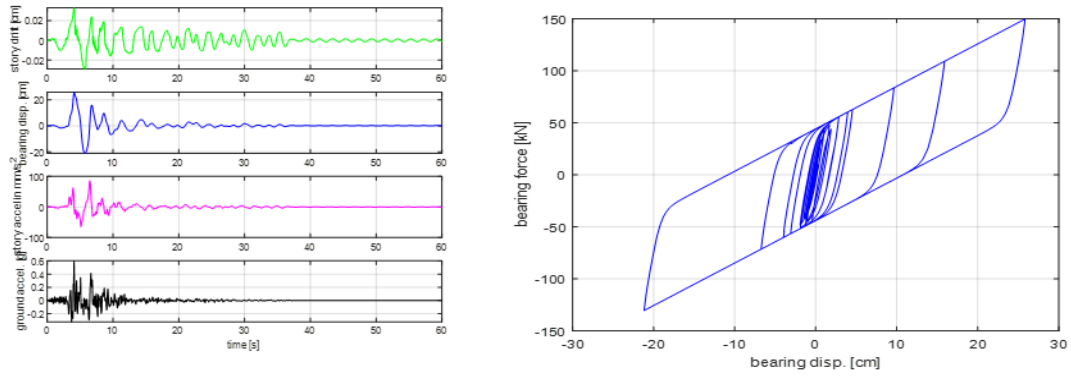


**Figure XLIX** The Structural Response with (LT6R) Under Northridge-01Ff, 90

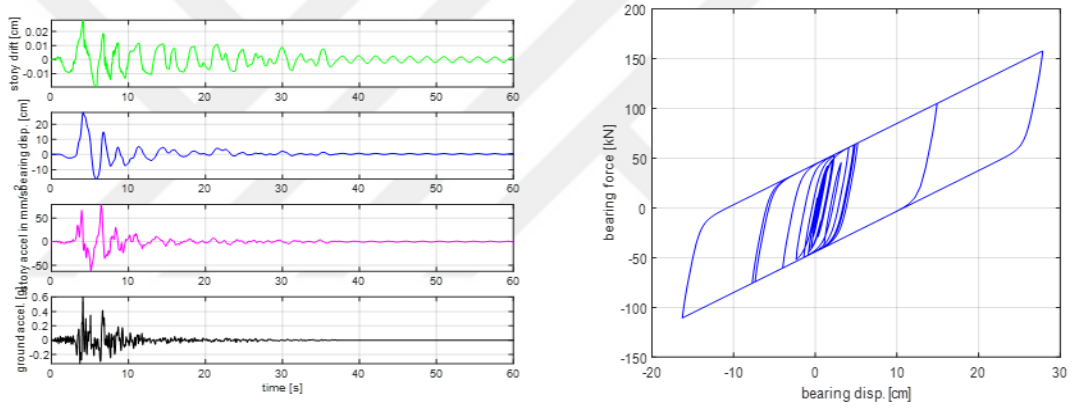


**Figure L** The Structural Response with (LT7R) Under Northridge-01Ff, 90

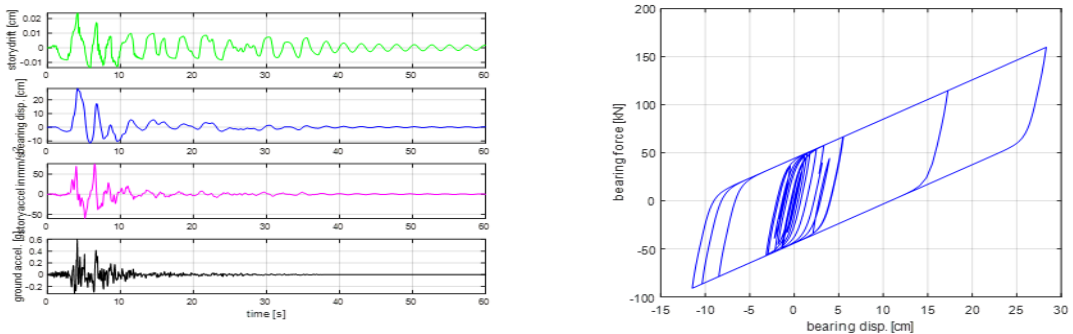


**Figure LI** The Structural Response with (LT8R) Under Northridge-01Ff, 90

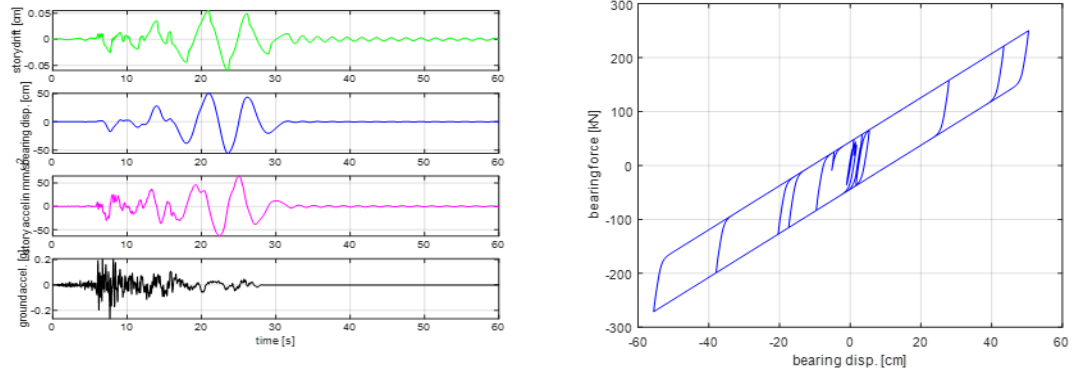


**Figure LII** The Response of Structure with LT6R to Cape Mendocino, 270

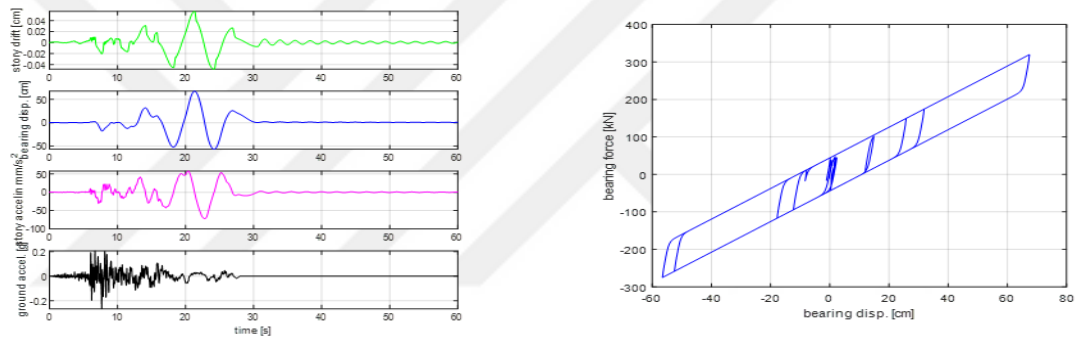


**Figure LIII** The Response of Structure with LT8R to Cape Mendocino, 270

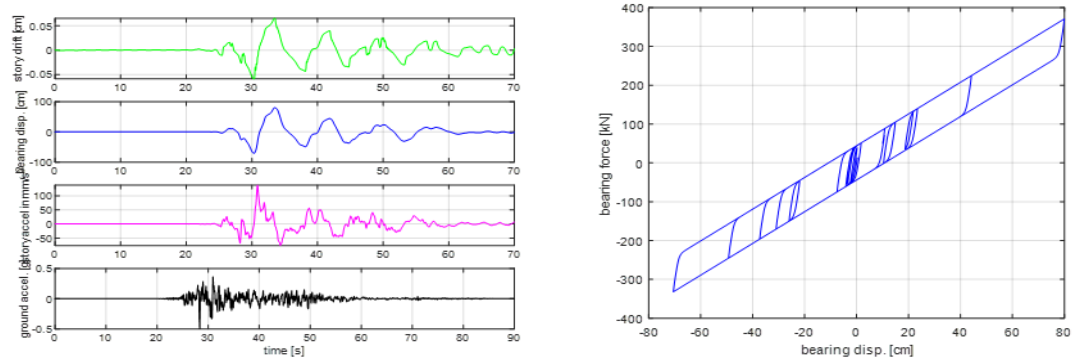


**Figure LIV** The Response of Structure with (LT6R) to Chi-Chi Tcu067, E

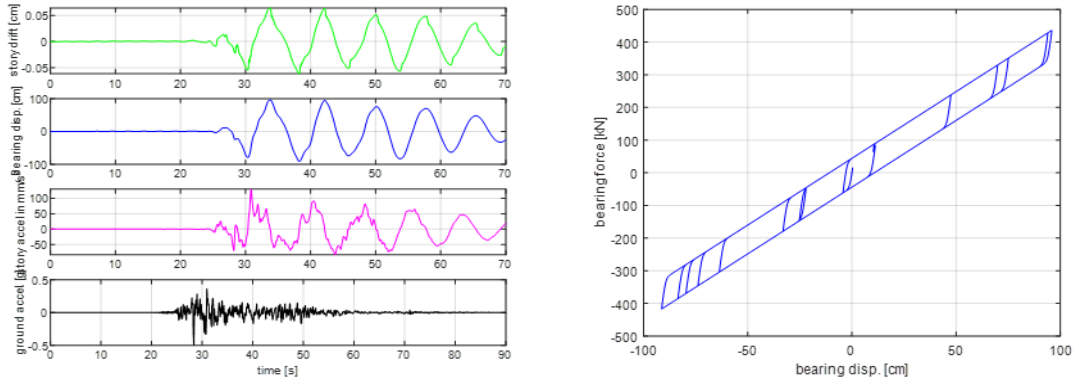


**Figure LV** The Response of Structure with (LT8R) to Chi-Chi Tcu067, E

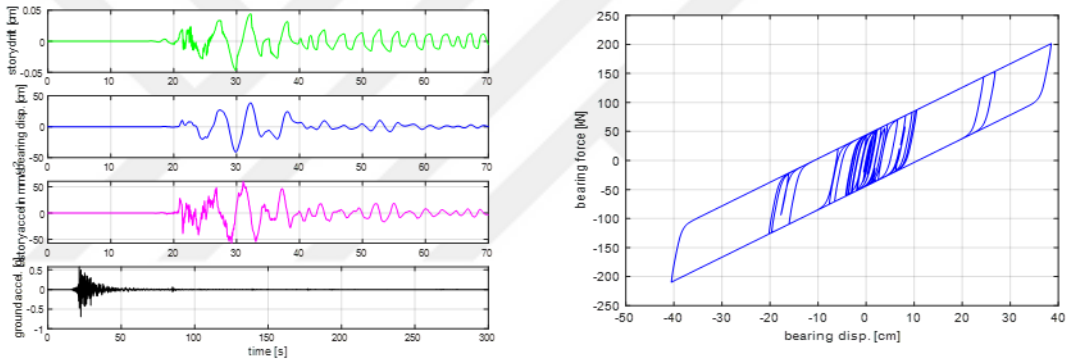


**Figure LVI** The Response of Structure with LT7R Against Iwate Myg004, Ew

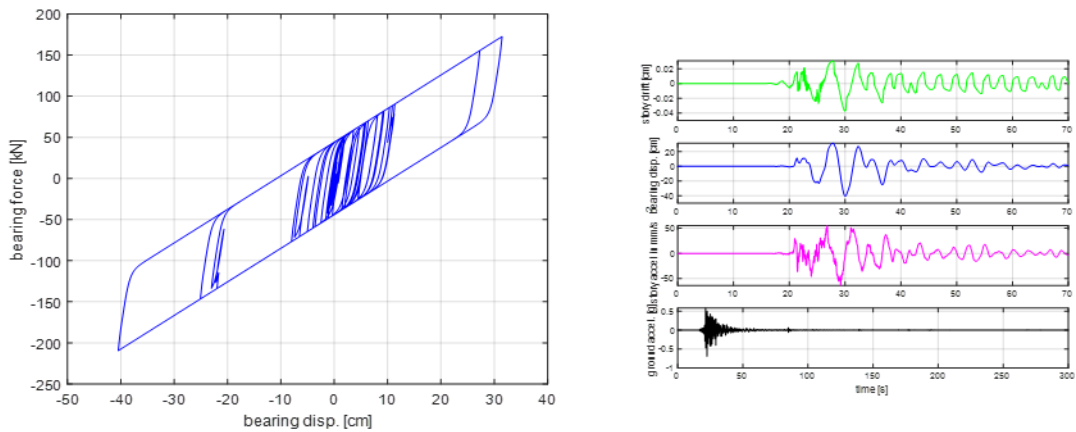


**Figure LVII** The Response of Structure with LT8R to Iwate Myg004, Ew